
Inertia and Rate of Change of Frequency (RoCoF)

Version 17

SPD – Inertia TF

16. Dec. 2020

1. Executive Summary	3
2. Introduction and Aim of the Document	4
3. Definitions	6
3.1 Inertia	6
3.2 Rate of Change of Frequency (RoCoF)	8
3.3 Centre of Inertia	9
4. Impact of Inertia on Power Systems	11
4.1 Frequency and Voltage Control of Generators	11
4.2 Stability	12
4.3 Protection Equipment	15
4.4 Short-Circuit Power	16
5. Criteria of Inertia Estimation	16
5.1 Regulatory Framework	16
5.2 Actual Status of State-of-the-Art for Inertia Measurement Methods: PMUs vs. SCADA	17
5.2.1 Use of PMUs	17
5.2.1.1 On-line Monitoring Based on Modulation Approach	17
5.2.1.2 On-Line Monitoring with “Significant Disturbance” Approach	18
5.2.2 Use of SCADA	21
5.2.3 Offline Inertia Monitoring and Forecasting	23
5.2.3.1 Overview of the different Methodologies	24
6. Simulations	28
6.1 Tools for Power System Dynamic Analysis	28
6.1.1 Model on Software Reference (MATLAB/Simulink)	28
6.1.2 Scenario Selection: Current and Forecasted Dispersed Generation)	30
6.1.3 Evaluating the Results of Simulations with the Reference Model	35
7. Methods to Increase and Support System Inertia	39
8. Challenges for the Future	41
9. Lesson Learned from the Current Power System Operation	43
10. Pragmatic Limit for Inertia and Rate of Change of Frequency	44
11. Conclusions and Recommendations	45
12. References	46

1. Executive Summary

The current document focus on the impact of the current and future consequences related to the power system dynamic behaviour based on a decrease of system inertia due to the stepwise decommissioning of generation units with rotating masses and their replacement by power-electronic connected generation. By analysing the corresponding behaviour of the Continental European power system, related recommendations can be extracted and considered for future developments.

Starting with theoretical considerations followed by practical approaches on how system inertia can be assessed, up to dynamic model calculation results, this report aims to give a guidance for power system engineers on the main factors and tools required in order to allow a comprehensive power system operation overview with respect to system inertia.

2. Introduction and Aim of the Document

Worldwide the generation mix within all power systems is in the middle of a dramatic transition. A general process of decarbonisation and phasing-out of nuclear power plants takes place.

The related classical generation of electricity is based on large turbo or hydro generator sets that, by their physical characteristics and without any further investment, make for a significant amount of inertia in the power system. That means, immediately after a loss of a significant part of power generation due to e.g. forced unit outages, the resulting system frequency drop is delayed by the inertia of overall rotating masses. This is of paramount importance, because a few seconds elapse before additional power reserves can be deployed to re-establish the power system equilibrium while remaining within acceptable frequency deviation limits.

Renewable generation is mainly based on PV or wind power infeed which is connected to the grid through power electronic interfaces and delivers, therefore, in principle no additional inertia to the power system. Consequently, the concern is that the resulting rate of change of the frequency (RoCoF) will increase to that extent that system security will be endangered. The response time of active power reserve activation or even emergency protection will be not fast enough anymore to stabilize the system.

The inverter-based generation is only one element of a complex mosaic; looking at **Figure 1** we can move from left and list four elements with a high impact on the electrical power systems: the extension of grids, that increases the complexity of interarea oscillations behaviour; the weather phenomena, more and more violent, that stress the electrical power system; the large power flows from periphery to the centre of grids; the market effects that create strong transients during change of the hours. In addition, we have to consider also the change of load behaviour, due to large diffusion of inverters, and also of the load control; all these elements, jointly with inertia decrease, raise the RoCoF absolute amplitude, on the one hand, and worsen, on the other hand, the frequency behaviour and damping of interarea oscillations.

Following the path of decommissioning of synchronous machines replaced by inverter connected generation, we can note two effects: the aforementioned decrease of inertia, but also short-circuit power reduction; the latter influences the impedance seen by generators, and thus affects the stability of the system and correctness of protection equipment operation. Moreover, here we also see the hidden relationship between active and reactive power: if short-circuit power is reduced (i.e. the impedance seen by generators is higher), the voltage dips are deeper and the perimeter of their influence is wider. A voltage dip may cause a commutation failure on HVDC links and, in general, disturb the correct operation of inverter-connected generators and loads; Concluding, a system with huge amounts of this kind of generation and load is weakened by reactive power phenomena and experiences active power transients.

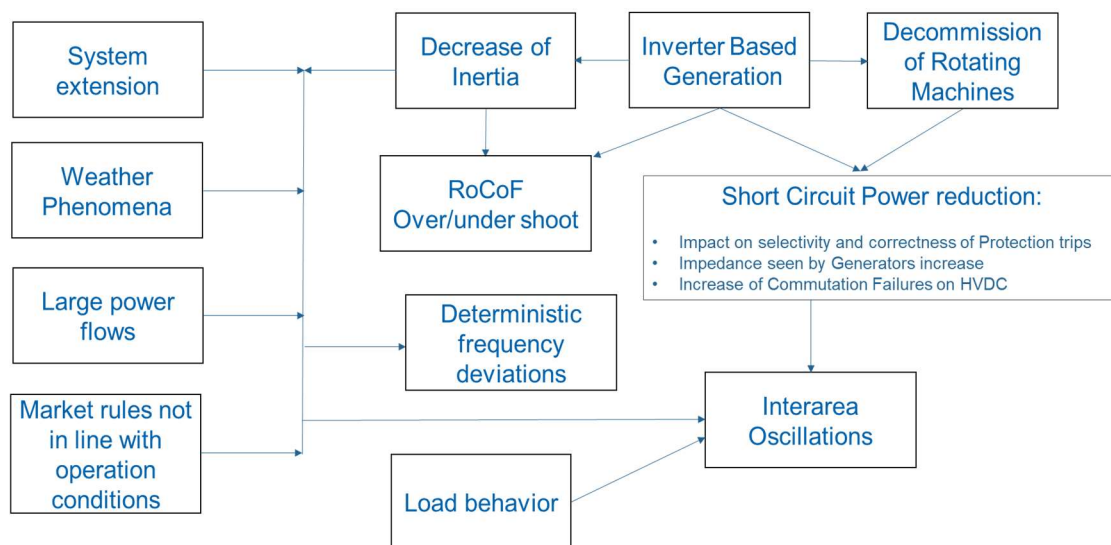


Figure 1 – Map of interaction

This document has not the ambition to describe all these complex phenomena. It rather focuses on inertia related issues by analysing in a comprehensive way the current state-of-the-art of coping with the above described challenges and explains the physical background as well as the existing equipment performances by using detailed information from dynamic modelling and current frequency measurement techniques. Therefore, the document deals with the problem of measuring the inertia level of an electrical power system and the most important indicator of its state of health from the point of view of frequency stability: the **RoCoF**. To fix a maximum RoCoF limit for an electrical power system means to determine the “maximum stress” that it can sustain and survive; this implies that under these conditions all the control loops, active power control and protection systems, including defence systems are able to trigger and react in accordance with their system governance settings .

In addition, the document illustrates direct and indirect methods to measure inertia, jointly with recordings of recent worldwide events reflecting how serious events were managed. At the end, some simulation results demonstrate and support the proposed feasible maximum RoCoF level for the Continental European power system.

3. Definitions

In this chapter we approach from mathematical point of view the main electrical concepts that are within the scope of the present document.

3.1 Inertia

Inertia definition directly derives from second Newton Law (“*Mutationem motus proportionalem esse vi motrici impressae, et fieri secundum lineam rectam qua vis illa imprimatur*”), expressed as in (3.1):

$$F = m \cdot a = m \cdot \frac{dv}{dt} \quad (3.1)$$

where F is resulting force [N], acting on a mass [kg] producing an acceleration a [m/s²].

Moving to electrical systems, the previous formulation refers to a mechanical mass rotating with a mean angular speed Ω [rad/s] and it can be expressed as

$$T_m(t) - T_e(t) = J \cdot \frac{d\Omega}{dt} \quad (3.2)$$

where $T_m(t) - T_e(t)$ represents the balance [Nm] between the mechanical torque impressed by a prime mover on the rotating mass and the electrical torque depending on the power exchanged with the system; the resulting torque, if different from zero, causes an angular speed deviation. Consequently, in absence of losses, we can assume that, in a physical electrical system, the inertia is an effect proportional to torque imbalance and inversely proportional to speed gradient. In formula

$$J = \frac{T_m(t) - T_e(t)}{\frac{d\Omega}{dt}} \quad (3.3)$$

where J is the total moment of inertia of the system, expressed in kgm². The same equation can be derived from another physical consideration; if we indicate the total kinetic energy of rotating masses with (3.4)

$$E_{kin} = \frac{1}{2} \cdot J \cdot \Omega^2 \quad (3.4)$$

The kinetic energy varies if a power imbalance is imposed to the system, so we can introduce a relationship between active power balance in the system and speed deviation:

$$P_m(t) - P_e(t) = \frac{dE_{kin}}{dt} = \Omega \cdot J \cdot \frac{d\Omega}{dt} \cong \Omega_r \cdot J \cdot \frac{d\Omega}{dt} \quad (3.5)$$

where we approximate the angular speed Ω with the rated one Ω_r [314 rad/s].

A more suitable quantity is the system equivalent inertia H [s], that can be defined as the ratio of the kinetic energy of rotating masses of the system and the rated power S [MVA] of synchronously rotating machines

$$H = \frac{E_{kin}}{S} = \frac{J \cdot \Omega_r^2}{2 \cdot S} \text{ [s]} \quad (3.6)$$

Proceeding by substitution, we obtain the equation (3.7)

$$P_m(t) - P_e(t) = \frac{2 \cdot S \cdot H}{\Omega_r} \cdot \frac{d\Omega}{dt} \quad (3.7)$$

and finally, considering that in power systems the best way to manage quantities is the pu (per unit) reference, i.e. by recalling the rated power reference of the entire system S , we can write:

$$p_m(t) - p_e(t) = 2 \cdot H \cdot \frac{d\omega}{dt} \quad (3.8)$$

or, introducing a new constant T , expressed in seconds and named “starting time”, we can rewrite (3.8) as

$$p_m(t) - p_e(t) = T \cdot \frac{d\omega}{dt} \quad (3.9)$$

Finally, we have to consider the relationship between starting time and inertia

$$T = 2 \cdot H \quad (3.10)$$

Coming back to the inertia, considering a group of N synchronous generators, forming part of a well-defined electrical area, assuming that it is islanded and the consumption is supplied only by synchronous generators, the Inertia Constant (in *seconds*) of the rotating machines can be represented as follows:

$$H_{syn} = \frac{\sum_i^N H_i \cdot S_{G,i}}{\sum_i^N S_{G,i}} \quad (3.11)$$

In order to take into account the effect of inverter-based generators, H_{syn} (3.11) has to be corrected by changing the reference basis¹ and re-formulating as follows:

$$H_{syn}^{gen} = \frac{\sum_i^N H_i \cdot S_{G,i}}{P_{LOAD}} \quad (3.12)$$

¹ Refer to formula (1) of “Frequency Stability Evaluation Criteria for the Synchronous Zone of Continental Europe” [8] (https://eepublicdownloads.entsoe.eu/clean_documents/SOC%20documents/RGCE_SPD_frequency_stability_criteria_v10.pdf)

The additional contribution of “M” rotating loads ($H^{load} = \sum_i^M \cdot H_i^{load}$) must be added to the inertia of the synchronous machines in order to represent the total grid inertia, expressed in seconds [s]:

$$H_T = H_{synch}^{gen} + H^{load} \quad (3.13)$$

The total kinetic energy (KE) stored in rotating machines (including loads) is defined by.:

$$KE_T = H_T \cdot P_{LOAD} \text{ [MWs]} \quad (3.14)$$

In some application we find as indicator of kinetic energy of the system the 4.14 formula with synchronous machines only:

$$KE_T = \sum_i^N H_i \cdot S_{G,i} \quad (3.15)$$

For the sake of simplicity, starting from now, we will refer to “H” to indicate total inertia of the electrical grid.

3.2 Rate of Change of Frequency (RoCoF)

Rate of change of frequency (RoCoF) is the time derivative of the power system frequency (df/dt): it is an important quantity that qualifies as the robustness of an electrical grid.

The initial value of the df/dt is the instantaneous RoCoF just after an imbalance of power in the electrical power system (i.e. disconnection of a generator/load tripping), before the action of any control. RoCoF is calculated as follows:

$$RoCoF|_{t=0^+} = \frac{\Delta P_{imbalance}}{P_{LOAD}} \cdot \frac{f_0}{2 \cdot H} \quad (3.16)$$

where 0^+ is the moment just after disconnection of the load/generation

As RoCoF is a time derivative quantity, it is important to define how to calculate it both in off line simulation studies (RMS) and from real measurands from the electrical system; general criteria and methods are reported in SPD document [11]. Again, it is worth noting that a wrong approach in calculating RoCoF can lead to erroneous evaluations or misunderstandings; in **Figure 2** we have an example of the effect of filtering selection on RoCoF evaluation: for “evaluator 1” the RoCoF in brown colour reaches peaks around +/- 2 Hz/s; for “evaluator 2” the same recordings show a RoCoF not exceeding +/- 0.2 Hz/s.

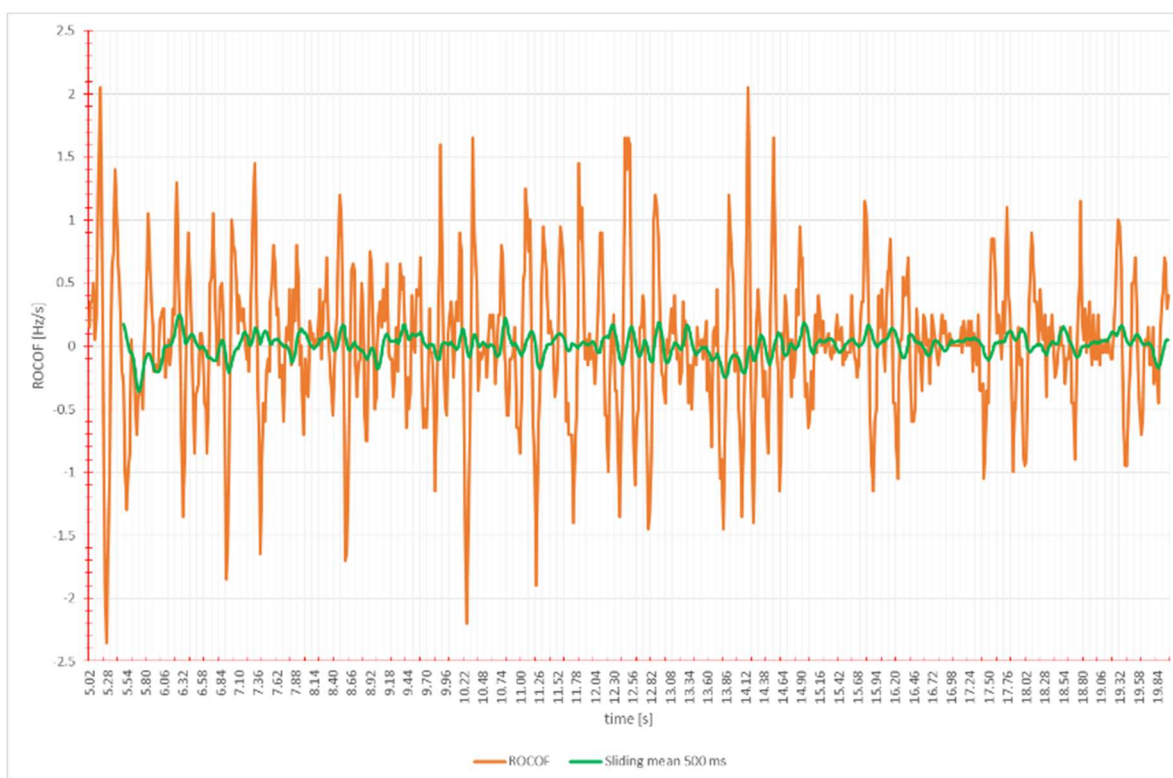


Figure 2 – RoCoF filtering (green colour) and un-filtered (brown colour) [11]

3.3 Centre of Inertia

The classical approach in studying electromechanical transients in a system is the nodal representation of the grid, describing with proper dynamic equations all the rotating machines and loads; on ENTSO-E site [10], a procedure is available to request this complete description of CE grid.

A complete nodal model has for output a simulation of N frequencies in physical selected busbars; it is evident also from real measurements (i.e. WAMs) that each measurand location has its local frequency, as reported in **Figure 3**.

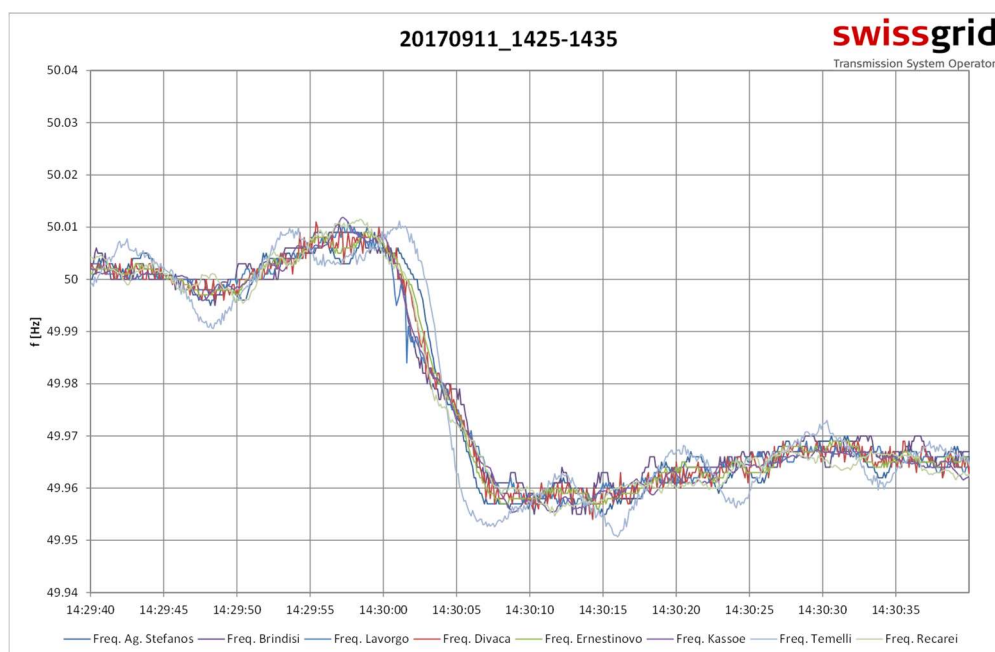


Figure 3: Forced Outage of 1000 MW Generation in Switzerland – PMUs recording (100 ms report rate)

In frequency transient stability studies, in order to describe the transient behaviour of a system with N generators, it is convenient to use the concept of Centre of Inertia (COI), defined as the inertial centre of all the generators. The position of COI (i.e. the rotor angle of the COI) is defined as follows:

$$\delta_{COI} \triangleq \frac{1}{H_T} \sum_{i=1}^N H_i \delta_i \quad (3.17)$$

where H is the sum of inertia constants of all N generators in the considered system and δ_i is the rotor angle of the generator with index i .

This approach simplifies significantly the study of the motion of a single machine (or of a cluster) against the entire system.

Considering the nominal power (in MVA) of the generators, the position of COI can be expressed as:

$$\delta_{COI_{Sn}} \triangleq \frac{\sum_{i=1}^N H_i \delta_i S_{n,i}}{\sum_{i=1}^N H_i S_{n,i}} \quad (3.18)$$

The COI has also an equivalent frequency that is:

$$f_{COI_{Sn}} \triangleq \frac{\sum_{i=1}^N H_i f_i S_{n,i}}{\sum_{i=1}^N H_i S_{n,i}} \quad (3.19)$$

4. Impact of Inertia on Power Systems

4.1 Frequency and Voltage Control of Generators

Synchronous generators provide frequency and voltage control to the system. In the following graph, the different power-frequency control loops established normally in a power system are depicted (taken from Policy 1 of Operation Handbook of UCTE) in Error! Reference source not found.:

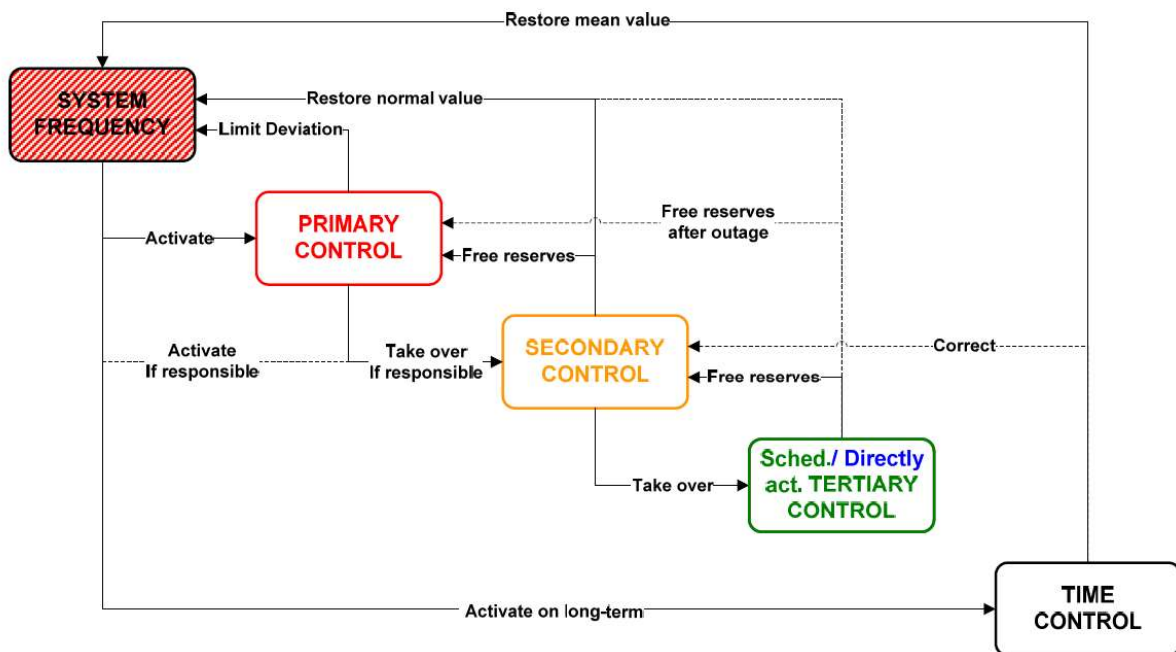


Figure 4 – Power-frequency control loops

While inertia softens frequency derivatives following a system imbalance through immediate and without any control actuation deployment of the energy stored in the rotating masses of the synchronous generators, the other power-frequency loops are based on controls. These controls involve different deployment times (from seconds to minutes or even hours) and require a careful coordination.

There is no factual impediment for renewable energy sources to provide these different power-frequency responses; but, as the mainstream technologies involved in the energy conversion from wind and sun (photovoltaics) to electricity are different from synchronous generators, the inertial capabilities normally involve only the generators.

The technologies that are used for this energy conversion from RES usually involve power electronics (Power Park Modules – PPMs) that, through very fast controls, are able to manage AC and DC power converters which allow transferring variable power input to the power system.

These power converters are able to synthesise the current wave following the voltage wave of the network in order to inject the required active power (grid following converters), which prevents these generators to show any natural behaviour towards frequency control. This behaviour, which would be similar to the inertial response of synchronous generators, can be obtained if the main control is changed from grid following to grid forming. These kinds of grid forming controls are

nowadays being extensively studied and tested, and they seem to be a promising technological advance in medium-term.

On the other hand, as the resource power (wind/sun) is variable and the control is scheduled at any time to produce maximum power, there is, in principle, no possibility for RES technologies to provide upwards reserves that would be given only if beforehand, the control is set to spill a certain amount of the possible power output. In addition, a certain reserve/storage capability is required in order to ensure a long enough time window of providing this additional amount of power.

In any case, RES technologies can provide different products of downwards power frequency reserves.

Finally, and even if the challenge is different, system inertia can be a parameter that also gives information about the system strength related to the different capabilities that, nowadays, synchronous machines and PPMs have.

In line with the influence of short-circuit power in the system transients, described in chapter 2, some considerations can be done about short-circuit power; although the present document focuses on inertia and related frequency issues, it is important to recall some concepts about reactive power too.

A synchronous machine is able to inject around 5 times its nominal current almost instantaneously when a voltage dip happens in the network nearby. This is a reactive power injection that helps the system recovering the voltage and, therefore, improves its transient stability condition. Taking into account that the current output is limited to the nominal rate of the power electronics of the converters (usually only slightly bigger than 1 pu), their response in terms of reactive power injection when voltage dips happen is limited (and it is, also, delayed by the needed control schemes). The difference of the behaviour between synchronous generators and PPMs can result in a notable worsening of the transient stability of the system.

New technologies of PPMs are able to provide static voltage control under similar conditions as a synchronous generator. This is not the case for older PPMs technologies, where voltage control is reduced to reactive power control, power factor control, or nothing at all.

4.2 Stability

A reduction of system inertia translates into a reduction of capability to damp oscillations.

The consequence of this reduction is a general worsening of transient stability performances of classical (synchronous) generating units when subject to small to large perturbations.

To illustrate this, the impact of reduction of inertia on the critical fault clearing time (CFCT) of a synchronous generator is analysed in this paragraph.

The CFCT is the most common criterion for the evaluation of transient angle stability. It is defined as the maximum time during which a disturbance can be applied without the system losing its stability².

With the help of a small example performed on a dynamic model, the main interactions are described below.

A large steam-driven synchronous generator is connected via its step-up transformer to a 380 kV busbar designated as Point of Common Coupling (POCC). The external system is modelled by two lines (series impedances) connected to an equivalent generator that represents the system strength before and after fault clearing (**Figure 2**).

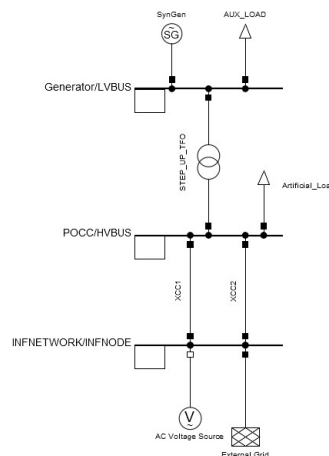


Figure 2 - SMIB system used to illustrate the impact of system inertia reduction on transient stability

The incident simulated is a three-phase metallic short circuit very close to the POCC that is cleared after 200 ms by opening the line with the lower impedance. This is equivalent to having a short circuit close to the unit that is eliminated by opening an important system branch that weakens considerably the system after fault clearing.

The same incident is simulated by reducing the system inertia from infinite inertia (ideal infinite voltage source) to a system with a respectively high, medium and low inertia.

It is important to note that the system strength is unchanged throughout the different simulations as well as the operational point and characteristics (except for inertia) of the generator in analysis.

The CFCT of a generator depends not only on system inertia, but also on the characteristics of the generator (intrinsic inertia moment, exciter and control tuning and characteristics, and system strength) and operational point.

² Determining generator fault clearing time for the synchronous zone of Continental Europe, 3 February 2017- https://eepublicdownloads.blob.core.windows.net/public-cdn-container/clean-documents/SOC%20documents/Regional_Groups_Continental_Europe/2017/SPD_FCT-BestPractices_website.pdf

For this reason, the results here have to be considered as qualitative ones only and are presented to illustrate the fact that a reduction of system inertia brings a reduction of CFCT and thus, in general, a reduction of the margin of transient system stability.

The simulation results are shown in **Figure 3**.

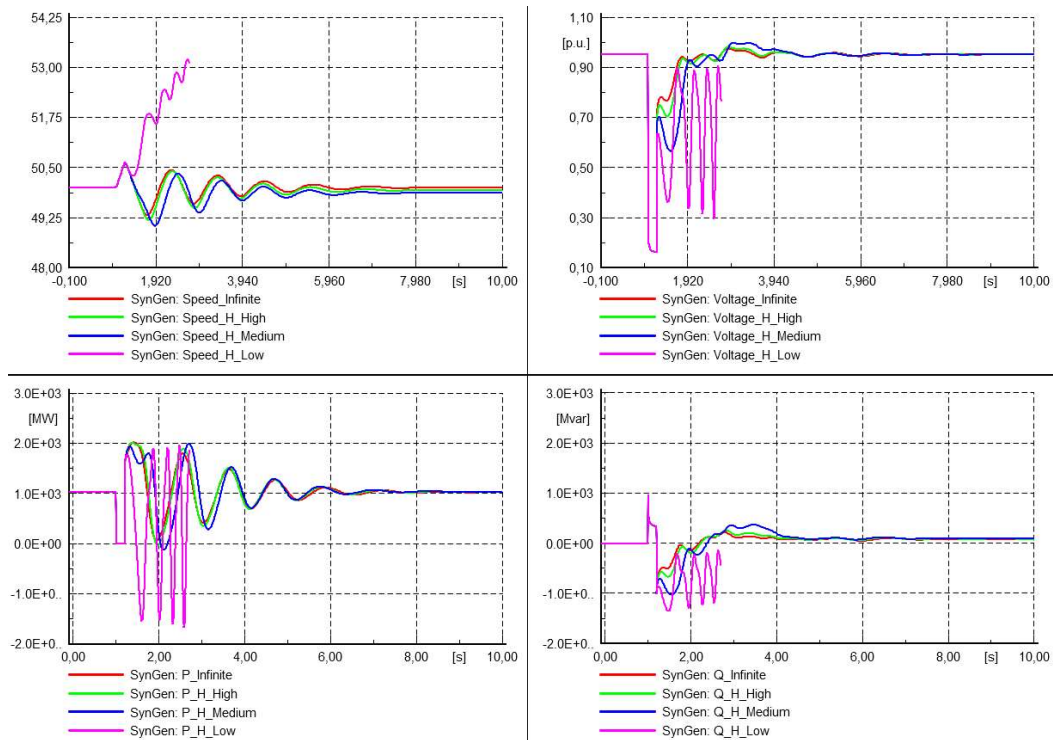


Figure 3 - Illustration of worsening of transient stability with system inertia reduction on a large synchronous generator. Top-left : speed in Hz, top right : stator voltage in p.u., bottom left : active power production in MW, bottom right: reactive power production in MVAR. Red/green/blue/magenta=Infinite / high /medium/ low system inertia

It can be noted that a system with infinite inertia (i.e. ideal) gives the best performances in terms of damping of this incident. When the inertia is reduced, the damping performances are also reduced. The generator will oscillate more and for a longer time for exactly the same incident. Eventually, with a low value of system inertia, the generator will become unstable and not trip in a timely way (with a possibility of being damaged), i.e. the CFCT is reduced below 200 ms.

It is also clear from the simulations that system voltage recovery, that is also a measure of system stability, is worsened with reduction of system inertia. A worsening of the voltage recovery may also have for consequence a cascading disconnection of other generators nearby the incident as the voltage at their connection points may be incompatible with the requested Low Voltage Ride Through characteristic.

The same incident in a system with lower inertia can have much worse consequences (e.g. disconnection of additional units) than in a system with higher inertia.

4.3 Protection Equipment

The electrical power system security depends on a reliable protection scheme. The proper functioning of the electrical power system protection must guarantee safety of persons and materials as well as continuity of electricity supply, limiting load shedding and avoiding a black-out. This protection system was initially designed to work in a grid with a high share of conventional generation (big synchronous machines centralized). The growing share of RES connected through power electronics in the electrical grid might have strong impacts on the protection system mainly because of:

- decrease of the global system inertia.
- decrease of short-circuit current injection.
- modification of electricity flows into the grid.

The focus will be here on the relation between the system protection equipment and the decrease of the global system inertia (increase of RoCoF, of frequency deviations and frequency variability).

As to safety of persons and materials, several devices are used for the detection and elimination of insulation faults in the transmission grid (current protection, differential protection, distance relays). The impact of the decrease of the global system inertia on the functioning of this equipment needs to be further studied.

The major issue related to the decrease of the global system inertia seems to be the risk of black-out or frequency collapse. To prevent a frequency collapse, the system is equipped with Under-Frequency Load Shedding (UFLS) relays that restore the production/consumption balance by shedding a portion of load when the frequency goes below certain thresholds. The majority of UFLS relays activates by reaching frequency thresholds only, but some of them are based on an additional RoCoF measurement and installed in some regions, particularly in grids facing high RoCoF and frequency variability such as French islands (Martinique, Guadeloupe). Indeed, the identification of a high RoCoF allows shedding more load preventively, before the frequency passes below the thresholds. The aim of all those emergency relays is to prevent the system from a frequency collapse.

When operating a relay and before tripping if a threshold is exceeded, the frequency and/or the RoCoF need to be measured. A frequency and/or RoCoF measurement produces a certain delay t_1 , and then the relay activation itself another delay t_2 . High RoCoFs could lead to three major issues sorted by criticality:

- Unintentional tripping due to inaccuracy in the measurement of the Frequency and/or RoCoF.
- Over extensive Load Shedding (due to the time delay of activation of the relays, the frequency falls below N thresholds corresponding to X% of the total load while shedding of Y% of load $\lll X\%$ would be sufficient),).
- Frequency collapse before the relays have time to trip.

Table 1. in chapter 4.4 in “Frequency Measurement Requirements and Usage” document provides guidelines on measuring the frequency within a time window allowing a accurate tripping of protection equipment [11].

A compromise has to be found between accuracy and measuring time window. If the measuring time window imposed to the relays is too large, the system will not be able to face high RoCoFs. The

requested measurement accuracy of protective relays can also be reconsidered to allow the system to face higher RoCoFs.

4.4 Short-Circuit Power

The capability of a synchronous machine to support the voltage and inject short circuit current is inversely proportional to its sub-transient reactance x_d'' . Both capabilities are linked though, however not in case of power electronics where a grid forming controlled inverter in can bring to the system a lot of voltage strength. but contributes only with a reduced amount of short-circuit current.

If no additional devices are inserted in the system (such as synchronous compensators), the global inertia decrease will be the consequence of replacing synchronous generators by sources connected through power electronics. Simultaneously, the capabilities of injection of short-circuit current and voltage strength of the system will be reduced. However, implementing grid-forming control in the power electronics could result in keeping the voltage-strength at the necessary level.

Installing synchronous condensers may bring both short-circuit current capability and inertia to the system. Moreover, a synchronous condenser has a more flexible design than a synchronous generator (regarding its H and x_d'' characteristics).

The actual protection scheme relies on equipment configured with thresholds defined for a system with high capability of short-circuit current injection. With the decrease of this capability this scheme needs to be continuously evaluated and at a certain moment adapted.

5. Criteria of Inertia Estimation

As the penetration levels of inverter-based generation resources (e.g., wind, solar, batteries) that do not naturally contribute with inertia to the system continue increasing and replace synchronous generators in the power system's generation mix, the synchronous inertia will inevitably decline, especially during operating conditions when the system load is low and wind and solar power production are high. These conditions vary depending on the season and time of the day. With these considerations in mind, it will become important for TSOs to monitor and forecast the system inertia in order to trigger adequate mitigation measures if it is expected to fall below a critical level.

5.1 Regulatory Framework

According to Article 39 of the Commission Regulation (EU) 2017/1485 (System Operation Guideline), TSOs of a synchronous area shall conduct a common study to identify whether there is a need to establish a minimum required inertia. Additionally, all TSOs shall conduct a periodic review and update those studies every two years.

If the studies demonstrate a need to define minimum required inertia, all TSOs from the concerned synchronous area shall jointly develop a methodology for the definition of minimum inertia required to maintain operational security and to prevent violation of stability limits. Each TSO of the concerned synchronous area shall deploy in real-time operation the minimum inertia in its own control area, in accordance with the results obtained with the approved methodology.

5.2 Actual Status of State-of-the-Art for Inertia Measurement Methods: PMUs vs. SCADA

The main difference between SCADA and PMUs data acquisition is the related time resolution. While in SCADA time resolution is in the order of seconds, in PMUs it is in the order of milliseconds. The higher resolution of Wide Area Measurement (WAM) systems allows transmission system operators noticing events that may have gone unnoticed using SCADA, such as inter-area power oscillations, etc. Another important capability of PMUs is the measurement, with a high level of GPS time stamp synchronization, of both the magnitude and angle of voltage and current, which makes it possible to carry out analyses that would otherwise not be possible using typical SCADA measurements. However, both devices can be combined for different applications, such as state estimation³.

5.2.1 Use of PMUs

5.2.1.1 On-line Monitoring Based on Modulation Approach

Different techniques are currently under study; the first approach is based on spectral analysis of the system frequency behaviour. This approach implies the injection in a grid node of an active power disturbance (sinusoidal or square wave or other cyclic signal) that stimulate the system to oscillate at a certain characteristic frequency. The injector device is, de facto, a sort of modulator in frequency and amplitude and could be an HVDC or battery or resistor bank properly controlled.

Knowing the input (the disturbance) and the outputs (frequency in different nodes) it is possible to identify the transfer function of the system and consequently estimate the inertia value (generators and loads).

The limits of this method are:

- The application is relatively easy for an islanded system, because the amplitude of the injected disturbance required to excite a proper frequency response of the grid could be reasonably small; a rather different problem would be the excitation of a grid oscillation over Continental Europe.
- An excitation of a mode over Continental Europe would induce power oscillations on tie lines that could disturb the neighbouring TSOs; in addition, this modulation could excite the inter-area oscillations. Therefore, proper verifications must be conducted.
- In an interconnected power system all tie lines must be monitored via PMUs in terms of exchanged power; this requirement clearly increases the costs as to number of devices, telecommunication links, etc.
- The approach is “small signal oriented”; in case of large disturbances it is not guaranteed that the estimation is correct,

³ NORDIC TSOs: https://eepublicdownloads.blob.core.windows.net/public-cdn-container/clean-documents/Publications/SOC/Nordic/Nordic_report_Future_System_Inertia.pdf

5.2.2.2 On-Line Monitoring with “Significant Disturbance” Approach

The second approach is more deterministic and bases the estimation on real time scanning of frequency in a way to identify “natural active power steps” (trips/manoeuvres of generation, loads, lines) that stimulates a frequency transient over the system. As transients are influenced by the available inertia, it is possible to estimate the latter via classical transfer function techniques or by applying more sophisticated algorithms.

As an example, a method⁴ of estimating effective inertia (i.e. taking into account all contributions to the inertial response) is being studied, which considers power imbalance as a time-varying function rather than a discrete step of power. Through subdivision into areas the centre of inertia of the investigated area can be identified. By using PMU measurements in the interconnection lines to the external system (i.e. external areas), this method integrates the power deviations between the time of the disturbance and the time t , representing the energy added to or removed from the investigated area across the boundary, up to time t . During a period when the system performs an **inertial response**, the **integrated power deviation and frequency shift are linearly related**.

The calculation of area inertia requires two main parameters: Rate of Change of Frequency (RoCoF) and power variation across the area boundary. The relationship between these quantities is provided by the previous mentioned equation (3.16) that can be written in this case as follows:

$$\frac{df}{dt} = \frac{\Delta P_{imbalance}}{P_{LOAD}} \cdot \frac{f_0}{2 \cdot H} \quad (5.1)$$

From equation above, more stable results are obtained by integrating both sides, as shown in the following equation:

$$\Delta f = \frac{1}{H \cdot P_{LOAD}} \cdot \frac{f_0}{2} \int_{t_0}^t \Delta P_{imbalance} \cdot dt \quad (5.2)$$

Where t_0 is the time of disturbance and Δf and ΔP_e are the “infinitesimal” changes of frequency and power through time, starting at time t_0 .

The integral is calculated for all time samples from the point of disturbance in time to a configured maximum time window. Therefore, the calculated inertia is a function of time. The algorithm finds the time samples with low variation in inertia and selects the minimum inertia value from them.

The method has been tested, with promising results, in both simulated and real environments. In order to ensure accurate outcomes, especially in large interconnections where disturbances rarely result in pronounced RoCoFs, further investigation is needed to:

- identify the time of the disturbance to use it as starting point,
- find the pre-disturbance level of frequency and power,
- evaluate the time window of the event necessary to ensure an accurate calculation.

⁴ See MIGRATE project - D2.3: Lessons Learned from Monitoring & Forecasting KPIs on Impact of PE Penetration

Among the methods for estimating inertia following a perturbation in the grid, techniques to reduce the network model to a dynamic equivalent are currently being studied⁵.

Considering the case of a typical electric power system with PMUs installed in N buses among the N_t buses (**Figure 4**), in order to apply the previously described methods, it is often necessary to **reduce the network to a dynamic equivalent**. In this regard, the **Ward method** can be used. Considering the figures below, in which a system with two areas and three PMUs is depicted, starting from the algebraic model of the power system, it is possible to construct the dynamic equivalent by defining the equivalent matrix Y_{EQ} (using the admittance matrix of the complete system) and compute the equivalent current injections I_{EQ} as:

$$I_{EQ} = Y_{EQ}V_R \tag{5.3}$$

Where V_R is the voltage vector.

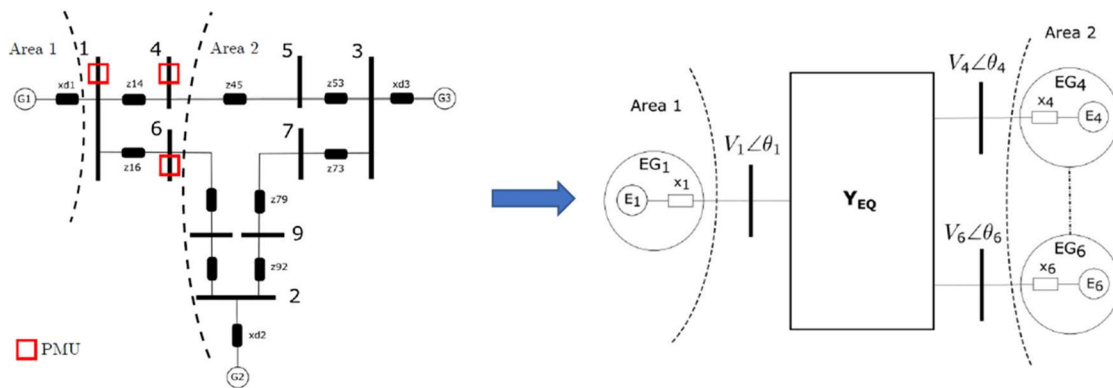


Figure 4 - Example of reduction of a network with N buses to a dynamical equivalent through the Ward method

With the knowledge of currents and voltage at the terminal buses of the equivalent generators, it is possible to estimate the transient reactances and then the internal voltages, which allows to compute, starting from the rotor angle, the frequency and the RoCoF.

Considering the **Figure 5** below, thanks to **PMU measurements** in points 1 and 2, it is in fact possible to obtain, by using algorithms such as the **method of variance** or the **Interarea Model Estimation (IME)**, the equivalent machine through which the network constituting an area is modelled.

⁵ See Moraes, G. R., Pozzi, F., Ilea, V., Berizzi, A., Carlini, E. M., Giannuzzi, G., & Zaottini, R. (2019, June). Measurement-based inertia estimation method considering system reduction strategies and dynamic equivalents. In 2019 IEEE Milan PowerTech (pp. 1-6). IEEE.

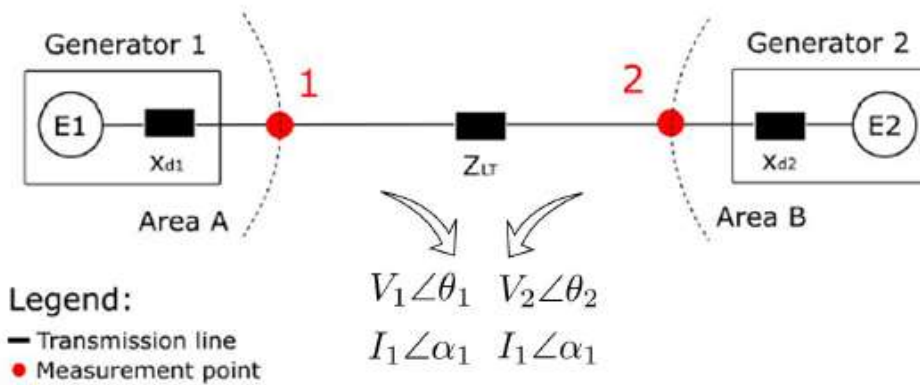


Figure 5 – Example of two generators connected by a line with Z_{lt} impedance

By exploiting the occurrence of a network event in area A, and therefore an imbalance in power $\Delta P_i(t)$, it is now possible to estimate the inertia of area B, and vice versa, by resolving the Swing Equations that we recall here:

$$\begin{cases} \frac{d\delta_i}{dt} = \omega_i - \omega_0 \\ \frac{2 \cdot H_i}{\omega_0} \frac{d\omega_i}{dt} = \frac{\Delta P_i(t)}{P_{LOAD}} - D \cdot (\omega_i - \omega_0) \end{cases}$$

where:

- δ_i is the rotor angle
- $\omega_i = 2 \cdot \pi \cdot f_i$ is the rotor angular speed
- D_i is the mechanical losses coefficient

Neglecting losses and reducing by substitution the angular speed in the Swing Equations, we obtain

$$\frac{H_i}{\pi \cdot f_0} \cdot \frac{d^2\delta_i(t)}{dt^2} = \frac{\Delta P_i(t)}{P_{LOAD}} \tag{5.3}$$

Considering a time interval around the perturbation under study, Equation (5.3) becomes an over-determined system that can be solved through the ordinary Least Squares method, by which the solution can be written as:

$$H_i = \pi \cdot f_0 \cdot (A_i^T \cdot A_i)^{-1} \cdot A_i^T \cdot \Delta P_i(t) \tag{5.4}$$

Where $A_i = \frac{d^2\delta_t(t)}{dt^2}$ and “T” represents the matrix transpose operator.

The results of the simulations carried out using test networks and applying the proposed methods are **promising**, as can be seen in **Figure 6**. Estimated frequency and RoCoF are very close to the real ones. The estimated values of inertia by **solving the swing equation with the method of least squares are very accurate**.

Some drawbacks of this method are:

- to apply the method, it is necessary to identify well-defined areas and the characteristics of the interconnection lines must be known.
- need for PMU measurements in some specific nodes of the network in order to identify dynamic equivalents.
- being an event-driven method, it cannot be used for continuous monitoring of inertia

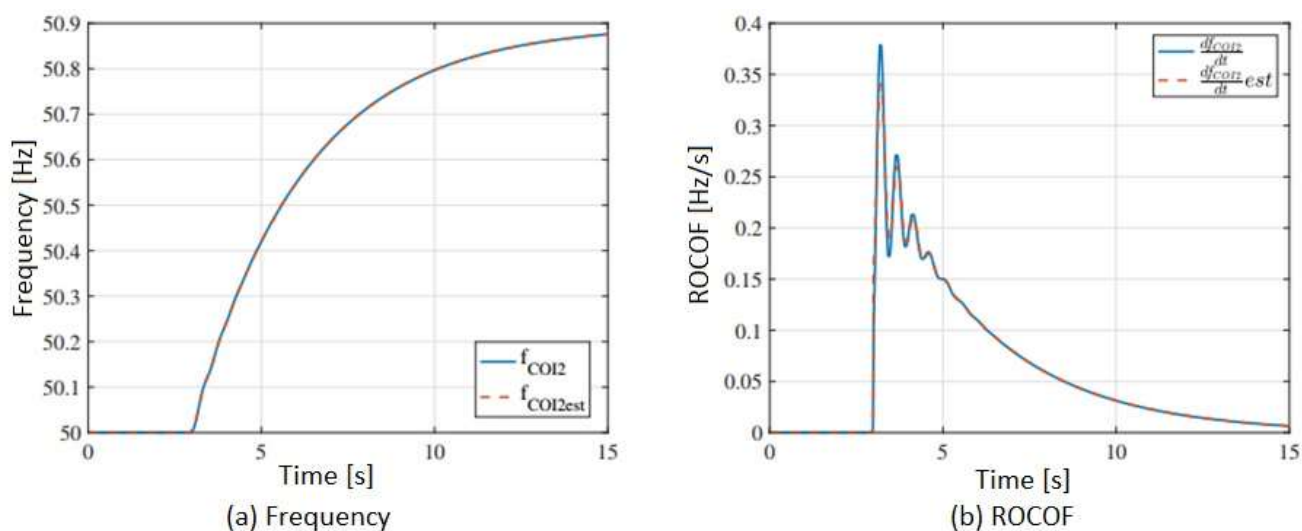


Figure 6 – Measured and estimated frequency and RoCoF with LS method

5.2.2 Use of SCADA

SCADA measurements can be used to determine the **inertia of the electric grid** by considering the **active rotating generators** (including synchronous condensers). Thanks to the widespread diffusion of remote terminal units (RTUs) used in the SCADA system, it is possible to constantly monitor the generators in service (this information is clearly also necessary for EMS systems). In order to determine the inertia of synchronous generators connected to the grid, the following information is needed:

- **Inertia** constant and nominal apparent power of each generator (technical data well-known by TSO)

- State of service (active/inactive) of each generator

While the information related to the first point is nominal data and, therefore, does not vary over time, the service status of the generators must be determined for each considered moment in time. This is where the SCADA system comes into play. It provides the status of the generators' circuit breakers and allows the determination of the set of generators in service with which to calculate inertia. The expression used for this calculation is the equation (3.11).

This method allows to continuously monitor the inertia provided by synchronous generators, giving a conservative indication (as the contribution of the loads and of other devices is not considered) of the amount of kinetic energy stored in the rotating masses directly connected to the grid. This information is also useful for correlation analysis of the trend of grid inertia with other characteristic quantities of the electricity system (e.g. total demand and Renewable Energy Sources (RESs) infeed). In **Figure 7** there is an example of inertia versus total demand and RES/total demand ratio on some typical days for the Italian power system, where a certain correlation can be observed in particular between RESs and inertia; the latter decreases when the RES production peaks. The scale in the right side of the y-axes is the same for total demand (GW) and RES/Total Demand (%).

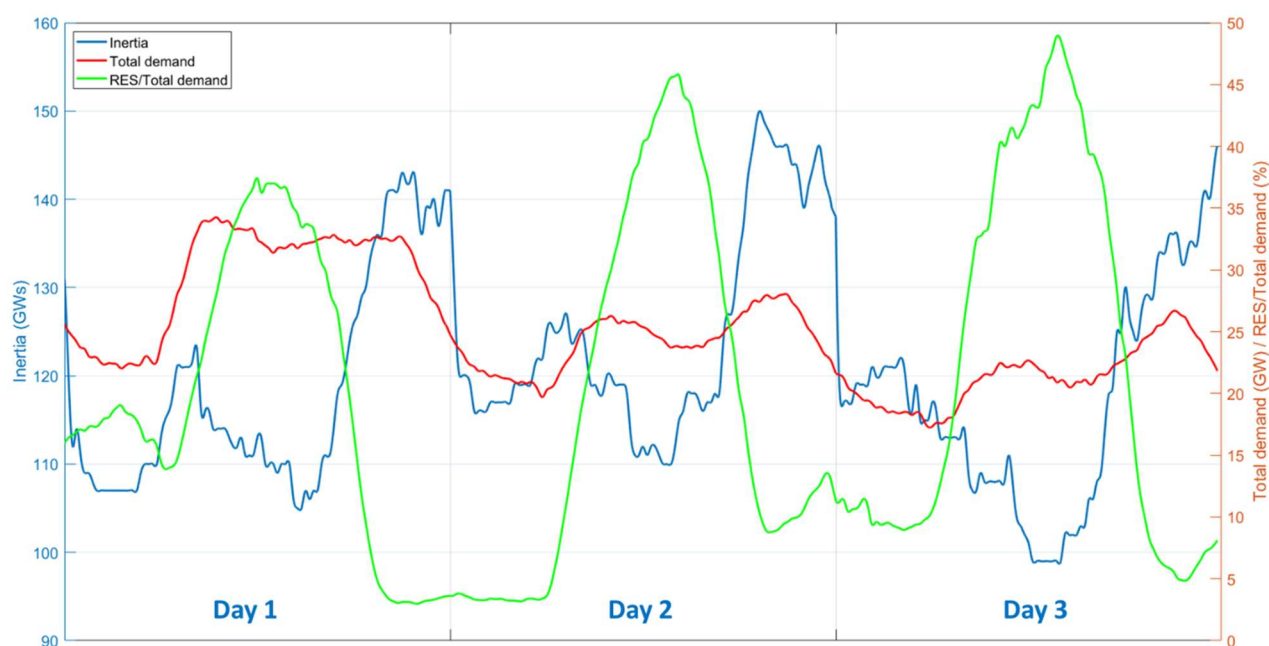


Figure 7 - Trend of inertia, total demand and ratio between RES and total demand of Italian system, during three typical days

The SCADA system can provide also the active power measurements of the interconnection lines between an area and the external system. This information can be used to determine the RoCoF of that area after its disconnection. The knowledge of the inertia of the disconnected area is also needed, information inferable from the rated values of generators or from on field tests.

On-line monitoring of RoCoF can be very useful to assess the frequency response of the grid following its disconnection from the external system. If the RoCoF reaches high values, countermeasures can be taken to reduce its magnitude, such as reducing transits in interconnection lines or increasing network inertia. For this reason, constant monitoring is important for network

operation. In **Figure 11** - ROCOF of the Italian system during three typical days there is an example of RoCoF trend on some typical days; this value assumes as system imbalance the total splitting of the area under monitoring. It may be noted that the absolute value of ROCOF is always below 1.5 Hz/s, calculated under the previous hypothesis of equivalenting the monitored area to one busbar model.

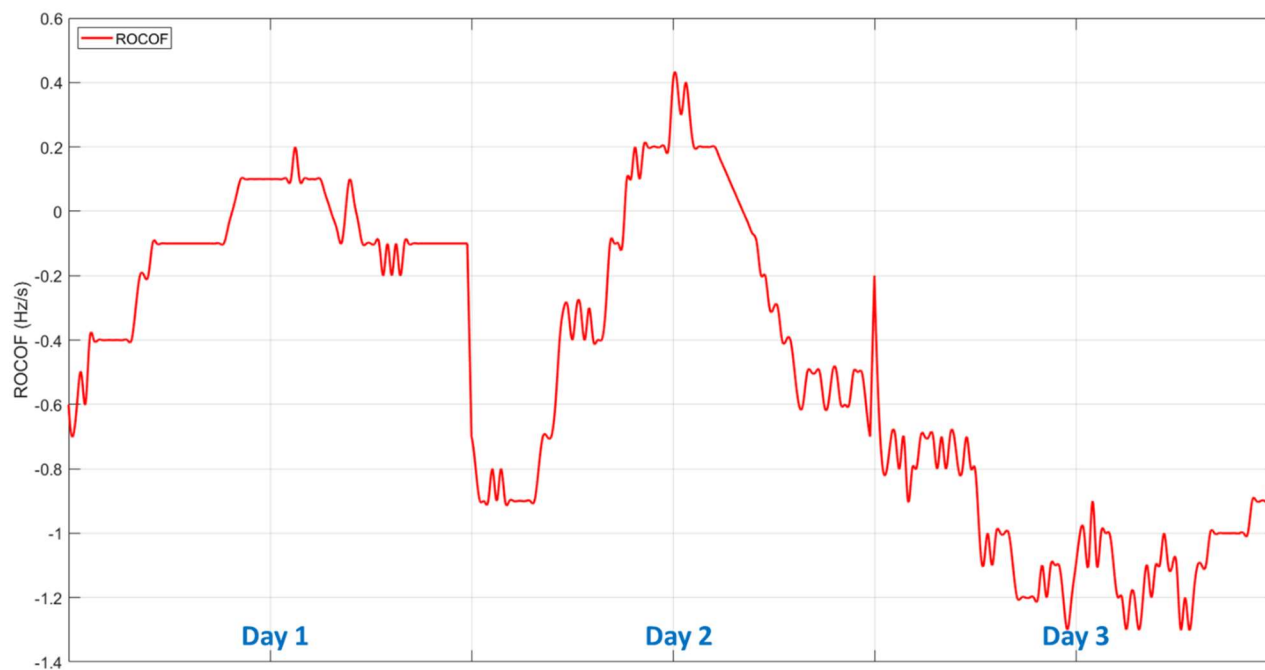


Figure 11 - ROCOF of the Italian system during three typical days

The methods based on SCADA data allow, therefore, an indicative calculation of the inertia and RoCoF of the network, but they also have some limitations:

- The type and sampling time of the measurements processed by the SCADA system does not allow the use of some of the innovative algorithms for the estimation of network inertia currently under development. On the other hand, the capillary diffusion of the measurements, currently covering broader regions than that of PMUs, allows a wider observability of the electrical system.
- For what has been written in the previous point, the inertia calculated with SCADA data does not consider the contribution of loads and other power sources (e.g. inverter-based RESs)
- The accuracy of the calculation depends on the quality of the SCADA system's remote signals and telemetry, as well as the accuracy of the inertia constant of the generators. For the most important installations in terms of their contribution to network inertia, however, the latter information is quite reliable.

5.2.3 Offline Inertia Monitoring and Forecasting

One simple way to derive estimations of the total system inertia/kinetic energy in a synchronous area system is to use the generation mix and basic assumptions about the inertia constant and loading factor for each generation technology. This section shows an analysis of the current total system

inertia/kinetic energy in the Continental European power system, taking into account the current status (year 2019) as well as the Ten-Year Network Development Plan (TYNDP) 2018 scenarios.

5.2.3.1 Overview of the different Methodologies

Different steps are followed in order to estimate the total system inertia within the Continental European power system. First, the hourly generation mix per production type (generation technology) is collected from the ENTSO-E Transparency Platform and the TYNDP 2018 scenarios. Moreover, typical inertia constants and loading factors (LF) for each production type are required as input (see formula 5.6) for the estimation. For Continental Europe, they are summarized in Table 1.

Table 1 – Typical inertia constants and loading factors for each production type

Production Type	Mean H [s]	Loading factor [-]
Nuclear	5,9	0,96
Fossil Brown coal/Lignite	3,8	0,81
Fossil Peat	3,8	0,59
Fossil Hard coal	4,2	0,70
Fossil Gas	4,2	0,60
Fossil Coal-derived gas	4,2	0,54
Fossil Oil	4,3	0,40
Fossil Oil shale	4,3	0,40
Hydro Run-of-river and poundage	2,7	0,61
Hydro Water Reservoir	3,7	0,56
Hydro Pumped Storage	3,5	0,46
Wind Onshore	0,0	-
Wind Offshore	0,0	-
Solar	0,0	-
Other renewable	3,5	0,50
Geothermal	3,5	0,83
Other	3,8	0,56
Waste	3,8	0,28
Marine	3,8	0,50
Biomass	3,3	0,70

In the first calculation step, an hourly weighting factor $w_i(t)$ is assigned to each of the n production types based on the overall generation mix:

$$w_i(t) = \frac{S_i(t)}{S_{tot}(t)} \quad (5.5)$$

The total system inertia $H_{sys}(t)$ and kinetic energy $E_{sys}(t)$ for each hour can then be calculated according to Equation (3.11)

$$H_{sys}(t) = \sum_{i=1}^n \frac{H_i(t) \cdot w_i(t)}{LF_i} \quad (5.6)$$

$$E_{sys}(t) = H_{sys}(t) \cdot S_{tot}(t) \tag{5.7}$$

Figure 8 shows the estimated total kinetic energy in Continental Europe for the year 2019. As can be seen, the total kinetic energy is influenced by the daily and seasonal demand pattern and the generation mix. Due to higher system load in the winter months, the mean total kinetic energy is usually higher compared to the summer months.

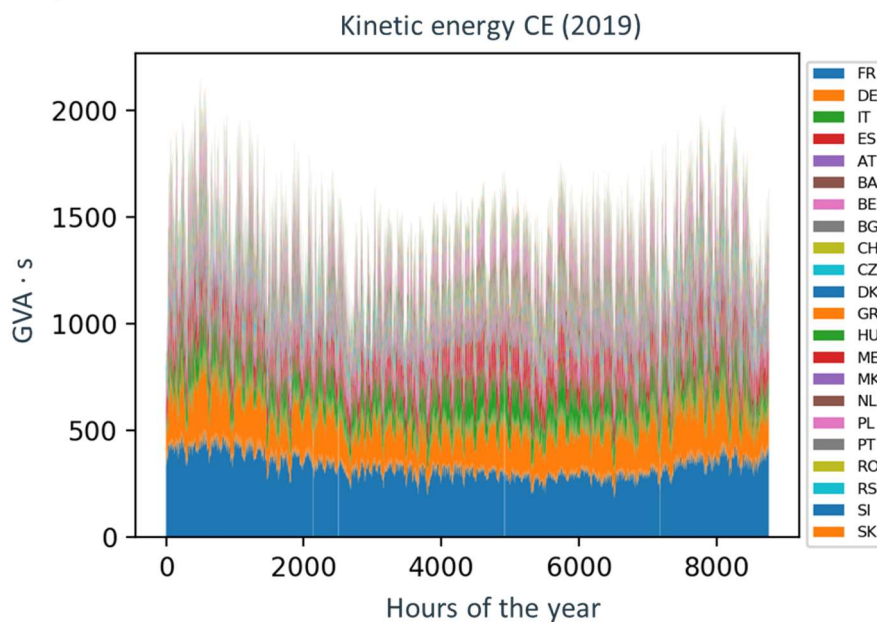


Figure 8 - Estimated total kinetic energy in Continental Europe

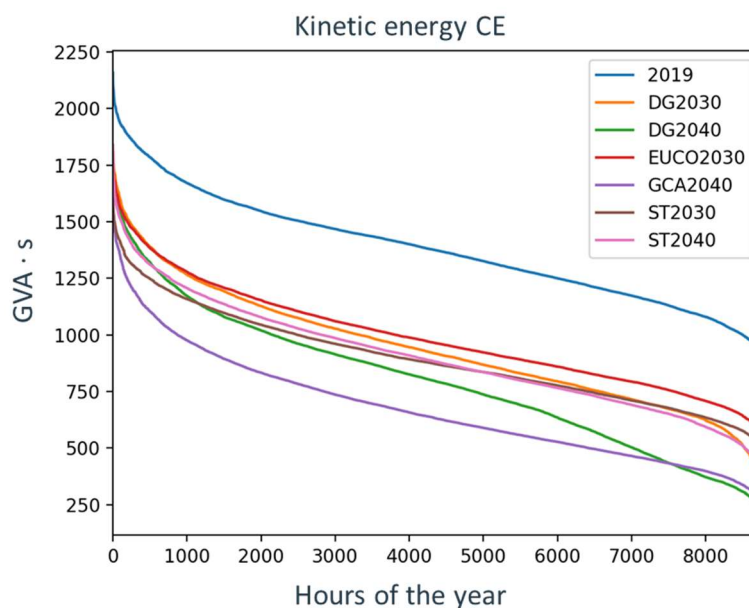


Figure 9 - Duration curves of the estimated total kinetic energy in Continental Europe

Figure 9 shows a comparison of the annual duration curves of E_{sys} for the years 2019 and the TYNDP 2018 scenarios. The duration curves display the share of time during which the kinetic energy is below a chosen value. As it can further be seen, the TYNDP scenarios show a significantly decreasing and slightly more volatile kinetic energy in the system. The decrease and the greater volatility of E_{sys} is directly linked to the increasing amounts of inverter coupled RES.

A detailed distribution analysis of the total system inertia in the year 2019 and in the DG 2030 scenario is shown in Figure 10.

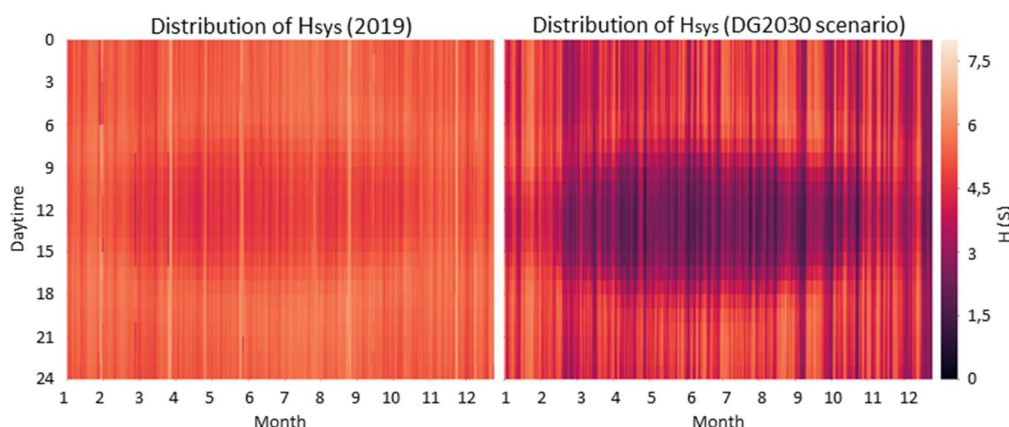


Figure 10 - Distribution of the total system inertia in the year 2019 and DG 2030 scenario

In the year 2019, a decrease of H_{sys} (dark spot in the center of the graph) is already slightly visible, which is mainly caused by the infeed from inverter-based photovoltaic (PV) installations. With the increasing number of inverter-based PV installations in the CE power system, this effect becomes

more evident in the scenario year DG2030. Furthermore, the pattern of Hsys in the scenario DG2030 additionally reveals dark vertical lines, which can be characterized as high infeed from wind power.

A simple working prototype for offline estimation of the total system inertia/kinetic energy in the Continental European synchronous area has been implemented. The estimations it delivers can be used to track the kinetic energy trend over time, and in future analyses.

However, there are uncertainties in this estimation associated with, for example, the data quality, the accuracy of the inertia constants or the loading factors. In order to improve the accuracy of the prototype, the estimated values must be compared against/validated with measurements, or more advanced estimation approaches need to be applied.

6. Simulations

This chapter deals with simulation calculations on a dynamic model to investigate the response of the power system to disturbances. The issue of system inertia falls primarily into the area of frequency stability. In terms of the latter, the disturbance is a power imbalance (the difference between the mechanical power of primary drives and the electric power of generators) and the response is a change of the network frequency.

6.1 Tools for Power System Dynamic Analysis

The purpose of dynamic analysis is to verify that the power system will not become unstable or even collapse during major disturbances, and to determine the operating limits of the system. There are many commercially available tools for the power system dynamic analysis. These tools use time domain for the frequency stability simulations and they enable modelling of the entire interconnected network. However, such a model is very complex. Somewhat simpler is the single-node model. Preparation, tuning and the calculation itself in time domain simulation tools is still a challenging matter. It still requires detailed models of generators and prime movers (especially turbines and their governors). Therefore, it was decided to use a proven balance model in the MATLAB/Simulink environment. This model is described in detail in the following part.

6.1.1 Model on Software Reference (MATLAB/Simulink)

An evaluation of frequency stability requires an analysis and assessment of the time-dependent system behaviour following power imbalances. For this purpose, an active power balance model in Matlab/Simulink was used, which is shown schematically in **Figure 11** and has been implemented and validated in previous studies.

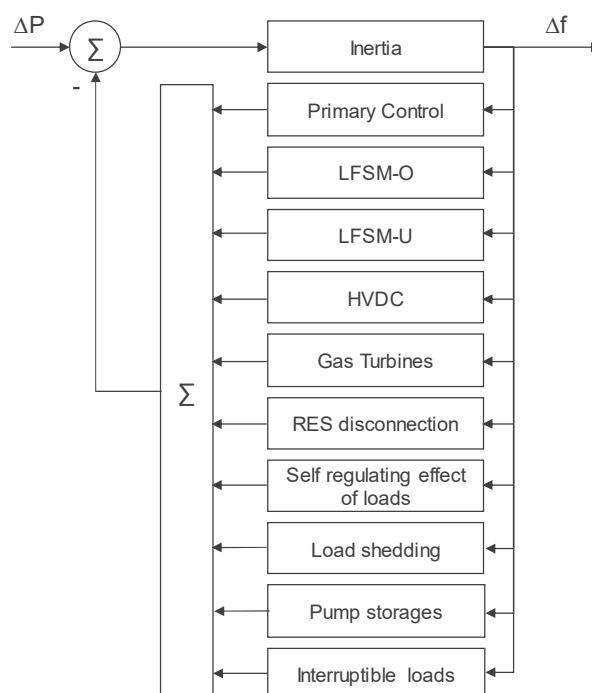


Figure 11 - Schematic block diagram of reference model in Matlab/Simulink

The balance model is based on an aggregation of all synchronous generators, non-synchronous generators and loads. Thus, the impact of e.g. voltage and angle deviations or power flow changes is neglected in this model. However, the aggregation allows the calculation of the time dependent system frequency (with respect to the centre of inertia) considering all modelled relevant frequency control mechanisms in the range of 47.5 Hz and 51.5 which have an impact on the dynamic behaviour and the frequency in particular:

- The inertia of the system is defined by the grid starting time T_a and is determined by the applied scenario.
- The primary control is modelled by a power terminal block PT1 with a time constant of 10 s and a gain of 30.000 MW/Hz, which is limited to a total primary control reserve of ± 3000 MW.
- LFSM-O, LFSM-U and frequency support by HVDC are modelled by PT1 block with a specific time constant and gain, in order to represent a frequency support above 50.2 Hz and below 49.5 Hz. For each unit individual limits can be defined. For the following simulations these control mechanisms are not considered, since they are not in system-wide usage at the moment.
- The decreasing power infeed from gas turbines at frequencies below 49.5 Hz is modelled with a gain of 10 %/Hz starting at 49.5 Hz. The active power drop due to frequency deviations is limited to a maximum of 3 % of the total infeed from gas turbines.
- The power consumption of electrical machines decreases during a frequency drop. This intrinsic self-regulating-effect of loads contributes to frequency stability and is modelled with a gain of 2 %/Hz for the 2020 scenarios and 1.5 %/Hz for the 2030 scenarios.
- In the range between 49 Hz and 48.1 Hz, a total of 8 different load shedding stages are modelled, each with a time delay of 100 ms representing the required time for frequency

measurement. For each stage 2.5 % of the total load is shed if the frequency threshold is violated.

- In the range between 50.2 Hz and 50.5 Hz as well as in the range between 49.8 Hz and 49.5 Hz four stages each are modelled, which represent non-grid-code conform RES units, which are disconnected at these frequencies. For each stage the installed capacity with the corresponding frequency thresholds is defined. With the use of a contemporary factor the infeed from non-grid-code conform RES (“NC-RES”) units for the specific scenario is set.
- In the range between 49.82 Hz and 49.2 Hz pump storages in pumping mode are either stopped or disconnected from the grid by opening the circuit breaker, in order to support the frequency. Therefore, the model contains 10 different blocks representing pumps disconnected by circuit breakers, which are shed immediately if the frequency threshold is violated. Another 10 blocks represent pump storages which perform a pump stop during 10 s and thus decrease their power consumption.
- Interruptible loads are modelled similar to the load shedding blocks and consist of 10 stages in the range between 49.82 Hz and 49.2 Hz, which are disconnected with a time delay of 300 ms.

6.1.2 Scenario Selection: Current and Forecasted Dispersed Generation)

This section presents the main scenarios and their underlying parameters, which are used for the simulations with the balance model. The main scenarios are derived from current observations (2020) based on ENTSO-E Transparency Platform data, dispersed generation data and the TYNDP 2020 scenario “National Trends” (NT2030).

Table 2 shows a comparison of the six main scenarios. The scenarios in 2020 and 2030 are further categorized in three sub-scenarios which include the following system conditions:

- High load (Figure 12 and Figure 15)
- Low load (
- Figure 13 and Figure 16)
- High RES (Figure 14 and Figure 17)

The chosen system conditions for each scenario are indicated by the orange dotted lines and estimated as follows from the time series data:

- High Load / Low Load scenarios:
 1. Search for hour X with highest or lowest load
 2. Extract generation mix and contemporary factors for hour X
- High RES scenarios:
 1. Search for hour X with highest share of RES
 2. Extract generation mix and contemporary factors for hour X

The main assumptions for the scenarios in 2030 are:

- Increase of system load (sector coupling, EVs, heating pumps, etc.)
- Decrease of network time constant T_A (increasing share of inverter-coupled generation)
- Decrease of self-regulating effect of loads SRL (increased share of inverter coupled motors/loads)
- Slight change of pumping contemporary factor (less pumping during low load; more pumping during high RES generation due to lower market prices) Decrease of the contemporary factor for the infeed from non-grid-code conform RES (NC-RES) due to retrofitting and new RES installations

Table 2 - Main scenario description

Year	Scenario	Load [GW]	PV [GW]	Wind [GW]	Gas [GW]	SRL [%/Hz]	Contemporary factor pumps [%]	Contemporary factor NC-RES [%]	T_A [s]
2020	High load	435	8.5	65	63	2.0	0	40	7
	Low load	200	6.5	18	9	2.0	45	10	7
	High RES	405	35.5	107	32	2.0	45	50	5
2030	High load	450	25	90	80	1.5	0	30	6
	Low load	200	10	40	10	1.5	40	5	6
	High RES	450	125	150	30	1.5	50	40	3

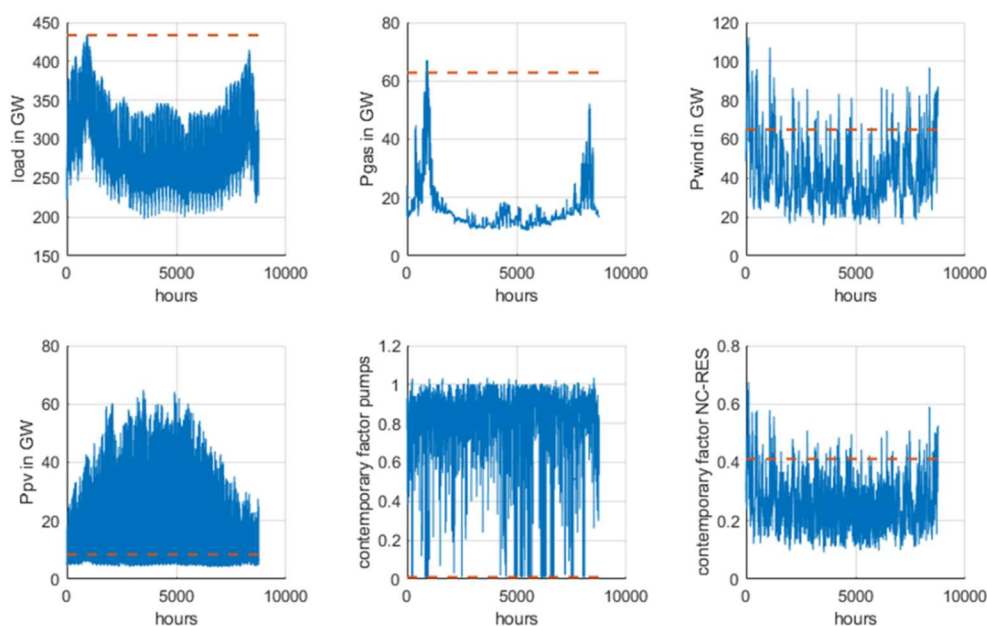


Figure 12 - High Load 2020

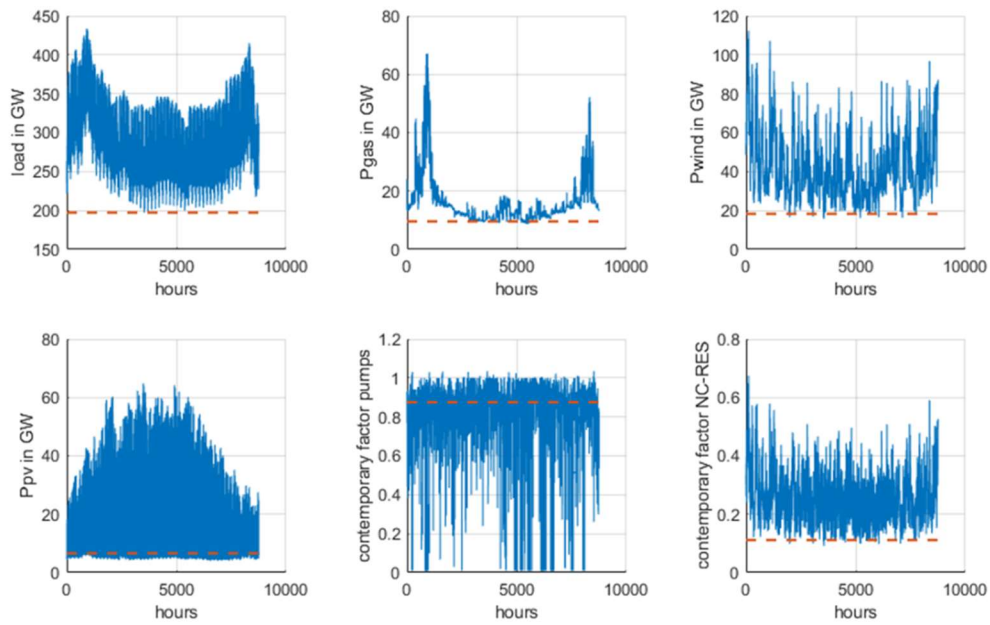


Figure 13 - Low Load 2020

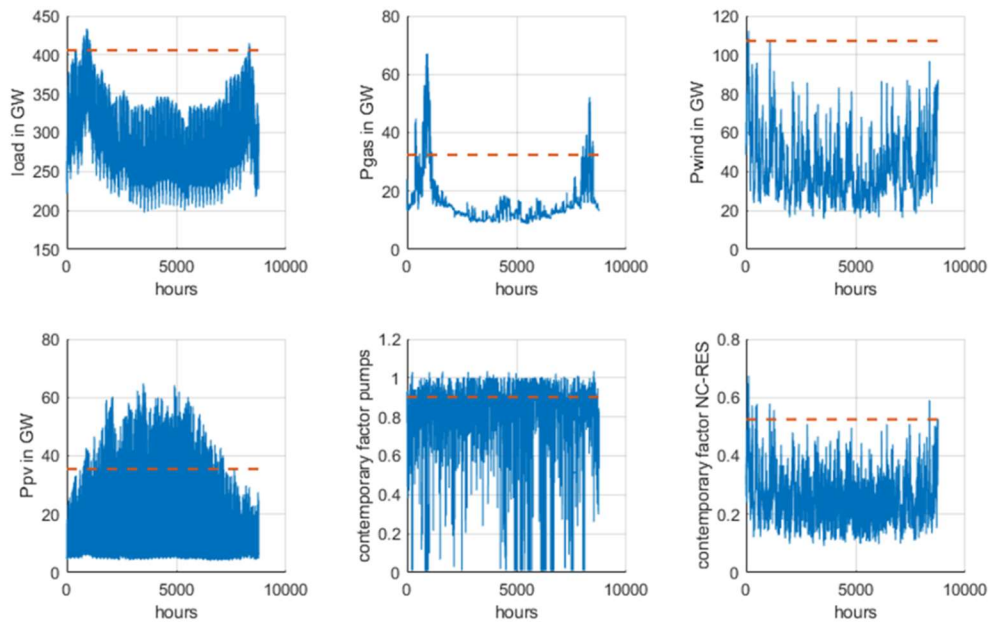


Figure 14- High RES 2020

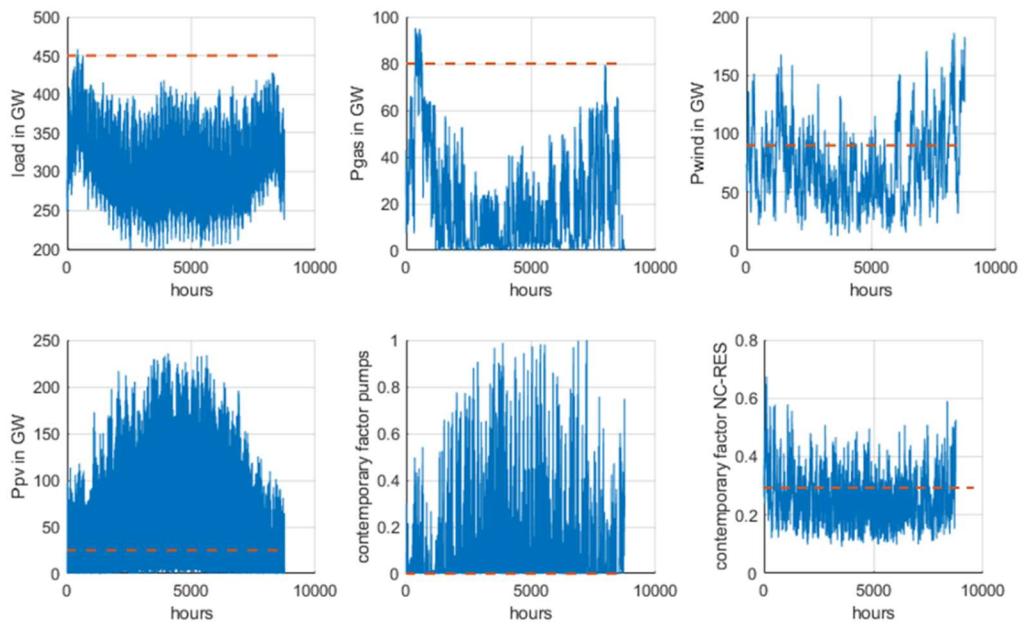


Figure 15 - High Load 2030

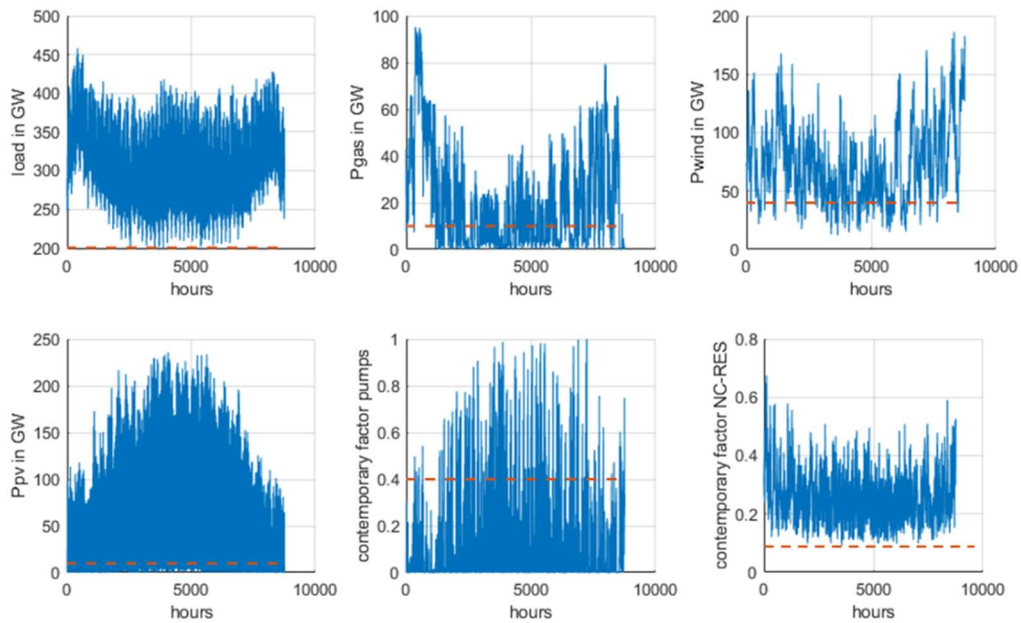


Figure 16 - Low Load 2030

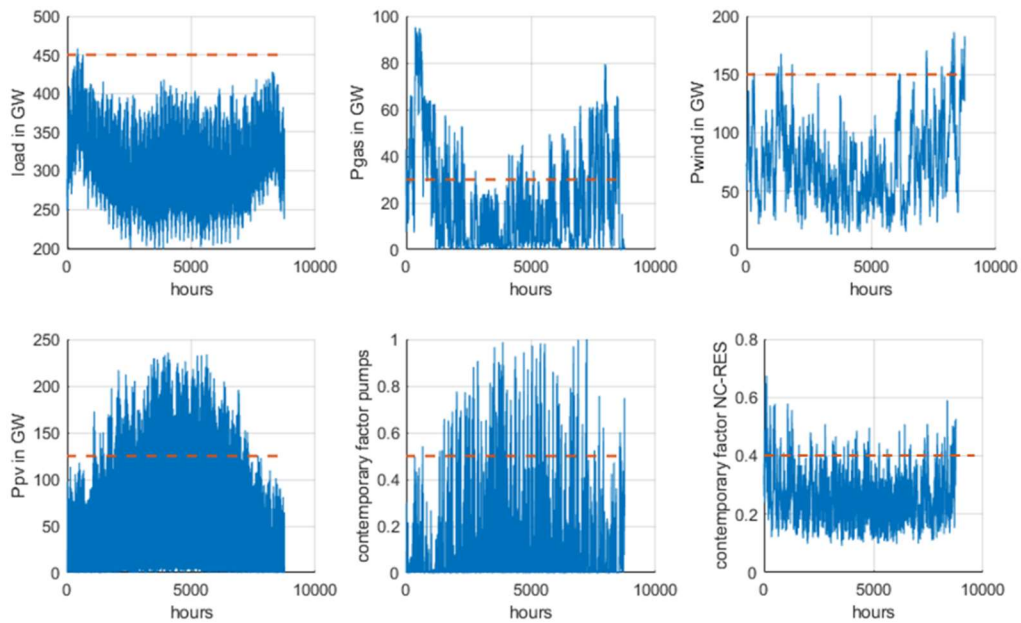


Figure 17 - High RES 2030

6.1.3 Evaluating the Results of Simulations with the Reference Model

In order to assess the frequency stability for the presented scenario framework, all three scenarios representing the years 2020 and 2030, respectively, have been applied to the active power balance model. In a first step, the low frequency behaviour is assessed by simulating a generation outage of 3 GW, which represents the dimensioning incident for the primary control in the Continental European power system.

Figure 18 shows the simulation results by means of the trajectory of frequency and frequency gradient for the high load scenario for 2020 and 2030. Due to the generation outage of 3 GW the frequency starts declining with a gradient of -0.05 Hz/s at first. Primary control as well as self-regulating effect of loads reduce the initial active power deficit and thus also the initial frequency gradient. Therefore, the frequency can be stabilized after approximately 30 seconds at 49.92 Hz for the 2020 scenario. By comparing the scenario for 2020 to the scenario for 2030 it can be observed, that the initial frequency gradient increases and the frequency nadir decreases due to the declining inertia of the system.

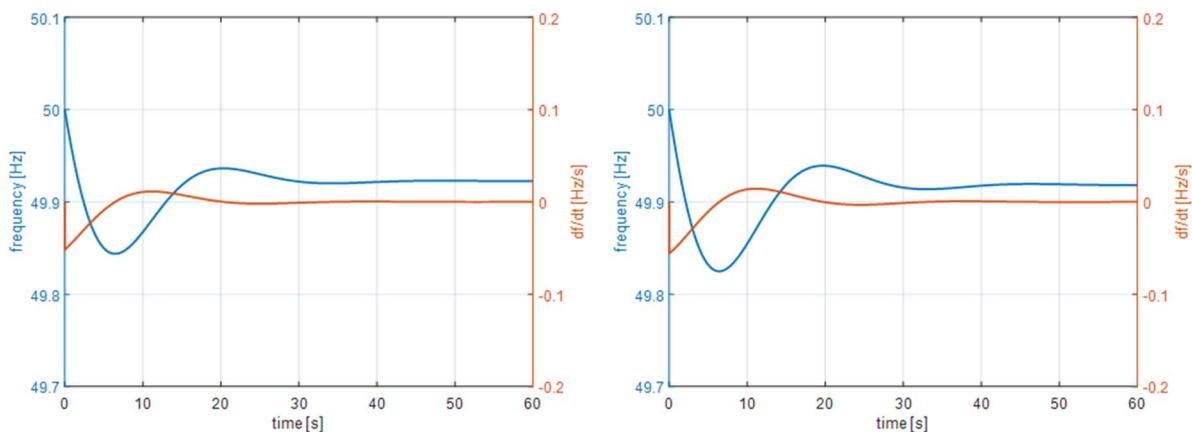


Figure 18 - Results for high load scenario 2020 (left) and 2030 (right) following a 3 GW generation outage

The simulation results for the low load scenario representing 2020 and 2030 are depicted in **Figure 19**. Again, the generation outage of 3 GW results in a frequency drop. Since the power deficit in comparison to the system load is significantly higher for these two scenarios, the resulting frequency gradient is much higher with -0.1 Hz/s. During the first seconds, primary control and self-regulating effect of loads reduce the power deficit and thus reduce the frequency decline. When the frequency reaches 49.82 Hz 1.5 GW of interruptible loads are disconnected after 120 ms representing the required time for frequency measurement. Following the disconnection of interruptible loads, the frequency starts raising until it reaches a steady-state frequency of 49.96 Hz. In comparison to the scenario 2020, the results of the scenario 2030 show an even higher initial frequency gradient due to the further decline of the system inertia. However, the frequency can be stabilized following the 3 GW generation outage due to the primary control reserves, self-regulating effect of loads, and disconnection of interruptible loads at 49.82 Hz.

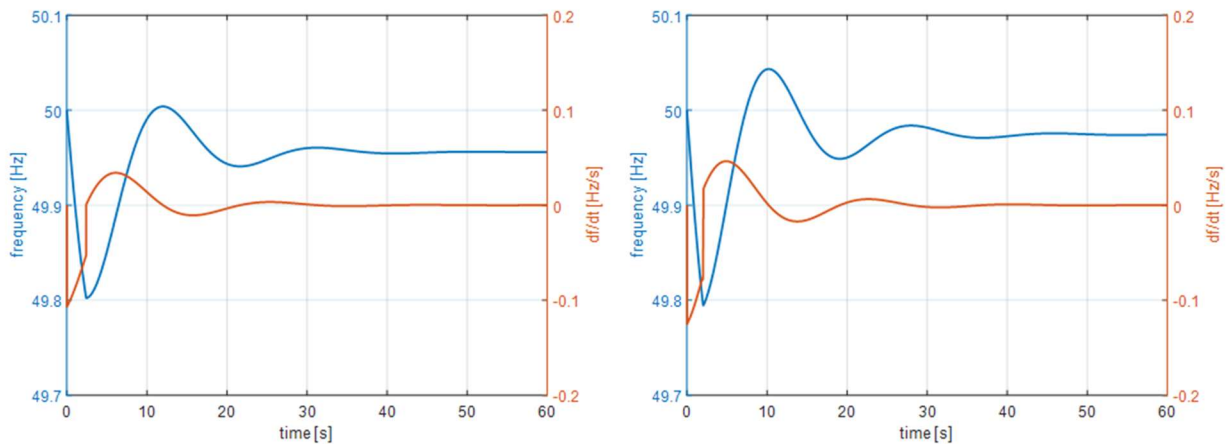


Figure 19 - Results for low load scenario 2020 (left) and 2030 (right) following a 3 GW generation outage

Figure 20 shows the simulation results for the 2020 and 2030 scenario with a high share of renewable energy sources, which also leads to a lower inertia compared to the system the results of which are presented in **Figure 19**. This also causes a higher initial frequency gradient following the 3 GW generation outage. For the 2020 scenario, the initial frequency gradient is approximately -0.75 Hz/s and the frequency is stabilized at 49.92 Hz. For the 2030 scenario, the share of RES is even higher, which causes the inertia of the system to further decrease. This causes an initial frequency gradient of -0.1 Hz/s and triggers the first stage of interruptible loads at 49.82 Hz as well as a disconnection of RES with an infeed of approximately 100 MW at 49.8 Hz. After triggering the disconnection of interruptible loads, the frequency returns to a steady-state value of 49.95 Hz.

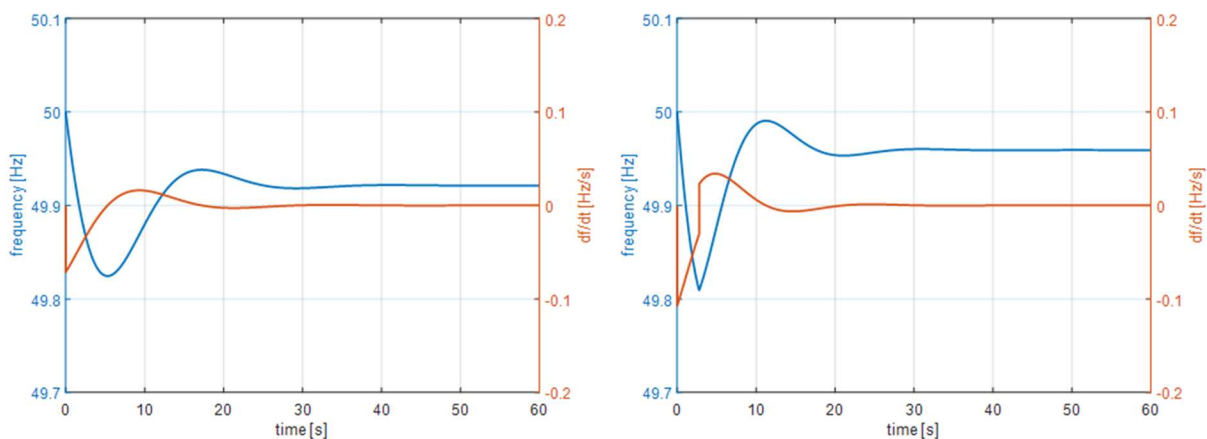


Figure 20 - Results for high RES scenario 2020 (left) and 2030 (right) following a 3 GW generation outage

In order to assess the system behaviour during over frequency events, a load outage of 2 GW has also been investigated, representing an outage of either an exporting HVDC systems or a large industrial load.

Figure 21 shows the simulation results for the high load scenarios in 2020 and 2030. In both scenarios the active power surplus in the system due to the load outage causes a positive frequency

gradient of approximately 0.05 Hz/s. Primary control and self-regulating effect of loads compensate the active power surplus and stabilize the frequency after 30 s at a steady-state value of 50.05 Hz.

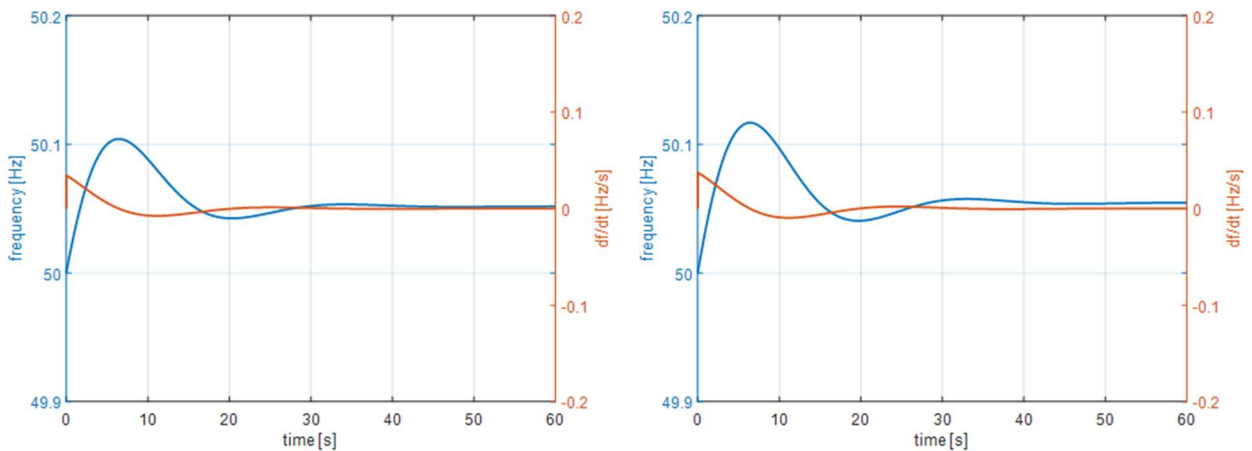


Figure 21 - Results for high load scenario 2020 (left) and 2030 (right) following a 2 GW load outage

Figure 22 shows the trajectory of the frequency and the frequency gradient for both low load scenarios following a 2 GW load outage. Since the active power surplus of 2 GW is proportionally higher than for the high load scenario, a steeper initial frequency gradient of 0.085 Hz/s can be observed in the 2030 scenario. Again, a slightly higher frequency gradient and larger frequency excursions can be observed, when comparing the 2030 scenario to the 2020 scenario. However, both scenarios show a stable behavior and the frequency is stabilized within 30 s at a steady-state frequency of approximately 50.05 Hz.

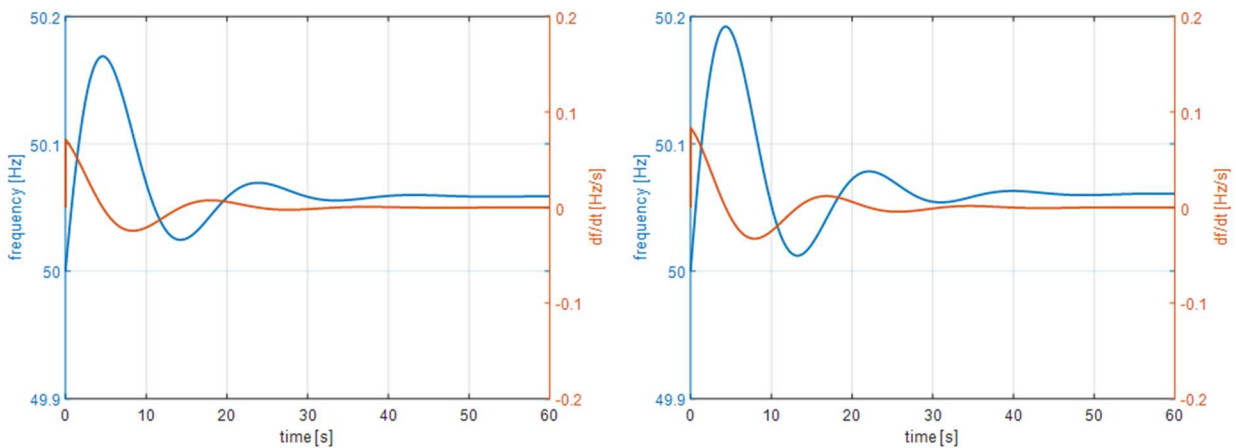


Figure 22 - Results for low load scenario 2020 (left) and 2030 (right) following a 2 GW load outage

Figure 23 depicts the simulations results for the high RES scenarios 2020 and 2030 following a 2 GW load outage. The resulting frequency trajectory is very similar to the results shown in **Figure 22**. Again, the initial frequency gradient as well as the frequency excursions increase for the 2030 scenario, due to the higher share of RES compared to the 2020 scenario, which finally results in a decrease in the inertia of the system.

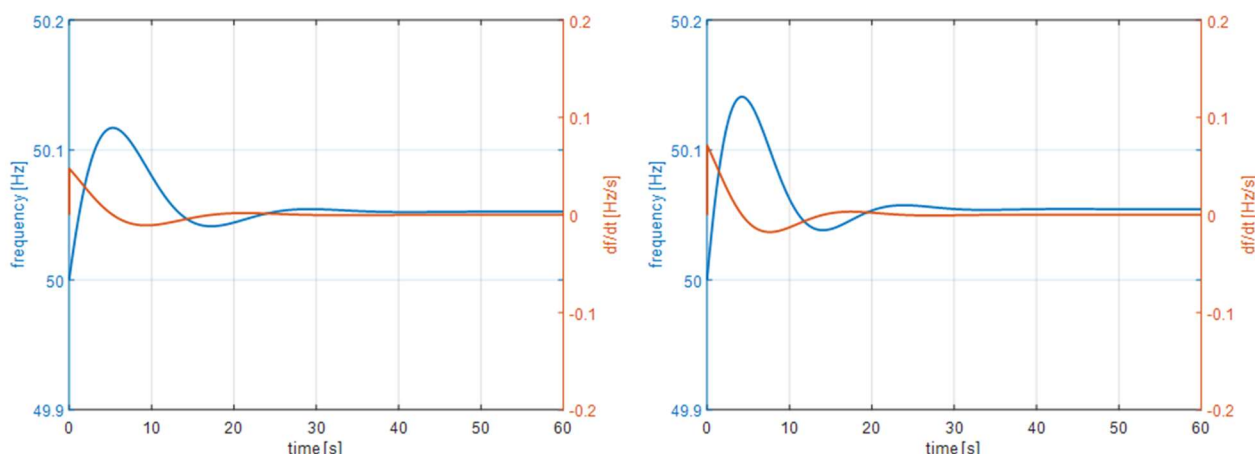


Figure 23 - Results for high RES scenario 2020 (left) and 2030 (right) following a 2 GW load outage

The simulation results presented in this chapter show a stable system behavior for all analyzed scenarios representing high load, low load and high RES scenarios for the years 2020 and 2030. Thus, it can be concluded, considering the progressive decrease of the system’s inertia due to increasing shares of RES, that generation outages up to 3 GW as well as load outages up to 2 GW can be handled today and in 2030 by the existing frequency control mechanisms.

The impact of non-conceptual incidents, such as system splits, has not yet been investigated so far and should be in the focus of further analyses, since a system split results in a larger frequency excursion and triggers additional supporting measures for stabilizing the frequency. In this context, interruptible loads, pump storages in pumping mode, gas turbines, load shedding schemes and disconnection of non-grid-code-compliant generation units play a crucial role and have to be examined considering the changing system characteristics.

7. Methods to Increase and Support System Inertia

In general, there are four ways of dealing with a deficit of inertia:

1. “Taking the risk”
2. “Reducing transit”
3. “Speeding up the control” and
4. “Increasing of system inertia”.

In the following, these four options, their usage cases and implementations are detailed.

“Taking the risk” means not taking any actions against the deficit of inertia. This is applicable when only out-of-range contingencies (i.e. no transient stability issues) and only relatively small parts of the system are affected. In this case, the out-of-range contingency probably leads to a local blackout, which is followed by a fast reenergisation under the support from a stable backbone of the main grid.

“Reducing transit” is referring to reducing transits across the AC-grid in order to keep imbalances after a system split within controllable limits. On the other hand, transits across HVDC links are not disconnected by system splits, and they are thus not contributing to the related imbalances. One of the most critical factors for potential high RoCoF is a too high transit power flow over long distances.

Therefore, reducing transits across the AC-grid is the most effective way to avoid instabilities in general. However, due to its the effect on the market, this approach should only be used when other means are not available or more expensive.

“Speed up the control” refers to the speed of over-frequency power reduction (LFSM-O) and other means like LFSM-U, load shedding and generation shedding, that are designed to reduce the dynamic frequency nadir and zenith. Those measures have an indirect effect on the averaged RoCoF over a given time window (most commonly 500 ms is analysed). They can only be implemented in long-term via network codes and find their limit, when:

- it comes to control the stability in a range of some 100 ms – here real inertia is needed– or
- the time for a sufficient quality of frequency measurement and reaction is exhausted. There is still room for optimization, i.e. by utilising choppers in case of over-frequency power reduction.

Examples for solutions using the “speeding up the control” approach might be:

- “Synthetic inertia” from wind generators is a new clever way to provide under-frequency response without permanent curtailment of the production. Besides the Alberta TSO demonstration with wind generators [(Demonstrating the Value of Wind Farm Inertial Response Functionalities to the Alberta Transmission System, 2020)] and good initiatives in Ireland [(EirGrid Grid Code Version 8, 2019)], the Hydro-Quebec experience with wind generators with this capability since 2015 have altogether proved that “synthetic inertia” from wind generators can reduce the nadir and RoCoF. However, due to the need to restore the pre-rotating speed of the blades, it causes a 2nd nadir and delayed frequency recovery. This concern is mainly associated with violation of operational criteria and UFLS operation

[(Asmine, Langlois, & Aubut, 2016)]. Delaying the time of blade speed restoration may reduce this risk.

- “Battery Energy Storage System for deployment of primary reserves (BESS)” based on lithium batteries have proved to be a good technical solution to provide fast frequency response and avoid using fast starting diesel generators in isolated systems, like islands. For Continental Europe, it is difficult to justify the usage of BESS economically, except in case of “second life batteries” whose “first life” is used for PV plants.

“Increasing inertia” can be achieved by TSO-measures or network codes. In medium-term, TSOs can install synchronous condensers with increased inertia or innovative STATCOM with storage capability. In both cases, synergies with measures for reactive power compensation are possible and sensible. Today, STATCOM with storage capability still rely on frequency measurements. However, with the fast developments in the area of grid-forming control, they will become an equivalent solution to synchronous condensers. Based on a further evolution of network codes, similar approaches as for the STATCOM can be applied to storage, converter-based generation and HVDC systems. This is not state of the art yet and, therefore, no application of Article 21 [1] of NC RfG or Article 14 of NC HVDC is known to the authors. Costs occur at adding (small) storages to devices, both for the storage itself and its internal connection via power electronics. Deriving a share of inertia from HVDC links interconnecting synchronous areas (or from HVDC links integrated in AC grids after a system split) is possible, but also not state of the art yet (manufacturers see only a mono-directional support as available today).

8. Challenges for the Future

For achieving the challenging targets towards a carbon neutral energy mix, a large amount of renewable energy sources will have to be installed.

As mentioned above, they are mainly inverter-based and nowadays equipped with a grid following control scheme and thus not contributing to the system inertia. Furthermore, they are often placed far from load centers, which results in much larger transits across the transmission system as we known today.

The following two developments worsen the situation in case of system splits:

- A larger transit across the network is transformed into larger imbalances in the separated islands.
- The inertia in the separated islands is decreasing.

According to equation (3.16) this leads to higher RoCoFs:

$$\text{RoCoF}_{\max} = \frac{df}{dt}_{\max} = \frac{\Delta P_{\text{Imbalance}}}{P_{\text{Load}}} * \frac{f_0}{T_N} \quad (8.1)$$

High RoCoFs mean that there is very little time for the dedicated automated schemes to reinstall the equilibrium between consumption and generation, which makes the remaining islands more prone to a blackout.

Side note: Large transits across the transmission system increase the risk of system splits significantly. As a consequence, it is reasonable to develop a concept for dealing with system splits. This is related to identifying the most likely system splits as well as looking deeper into the control schemes (system protection schemes) that are designed for stabilizing the resulting islands.

Which are the elements for making the system future-proof in terms of resilience against system splits?

As illustration, the options depicted in chapter 7 are assessed against their applicability for the future system design in the theoretical case of a system split:

1. “Taking the risk” is only appropriate for system split scenarios that result in relatively small islands that can be re-energized quickly. Here, the costs for preventing a blackout are unreasonably high compared to the damage that a blackout may cause. In this context, it has to be considered that a system split is a very rare event.
2. “Reducing transits” may be an exceptional option during the transitory time span when no other option is available. For the design of the future system, it is no option, because it would inhibit the transition towards a carbon free energy mix.

“Speed up the control” is a very elegant option, since it is related to low costs. It mostly optimizes the technical capabilities of different technologies and schemes. The more of this potential can be tapped, the higher is the value of the maximum admissible RoCoF. For sure, a precondition is a consolidated technological capability and sufficient operating experience.

3. “Increasing inertia” is the option for system split scenarios leading to islands of significant size, where a fast re-energization after a blackout is not possible. If grid forming control schemes are applied on inverter-based generation or other inverter-based devices, the number of devices that needs to be installed for the sole purpose of increasing the system inertia can be reduced. It should be investigated which share of the required inertia can pragmatically be provided by devices with grid forming capabilities, and which one by dedicated network-based assets. Also, this technical challenge has to be sufficiently investigated and experienced on field.

Success factors for mitigating system splits in future networks:

1. Speed up the control as fast as possible. This is resulting in a high admissible maximum RoCoF.
2. Roll out grid forming capabilities on inverter-based devices in order to reduce investments in devices that are only dedicated to deliver inertia.
3. Install network-based assets that provide inertia.
4. Make sure in real time operation that inertia and devices with grid forming capabilities are evenly distributed across the whole system in order to avoid high local RoCoF values (inertia must-run).

9. Lesson Learned from the Current Power System Operation

The aim of this chapter is to support deducing the RoCoF limit value based on serious events within the CE power system and one extreme event outside; in order to support the argumentation, WAMS measurands with a sufficient precision are used.

Looking at **Figure 24** we can note that related events are arranged into two groups – in the upper ones, the CE interconnected system survived in a stable way; in the lower ones, the entire system was or parts of it were blacked out. As key factors, the imbalance ratio before the event happened as well as the RoCoF for the center of inertia can be extracted.

Coming back to the upper part of the figure, we can see that for different imbalance ratios we face different RoCoF values, in any case lower than 0.5 Hz/s; in all events the defense systems were able to trigger.

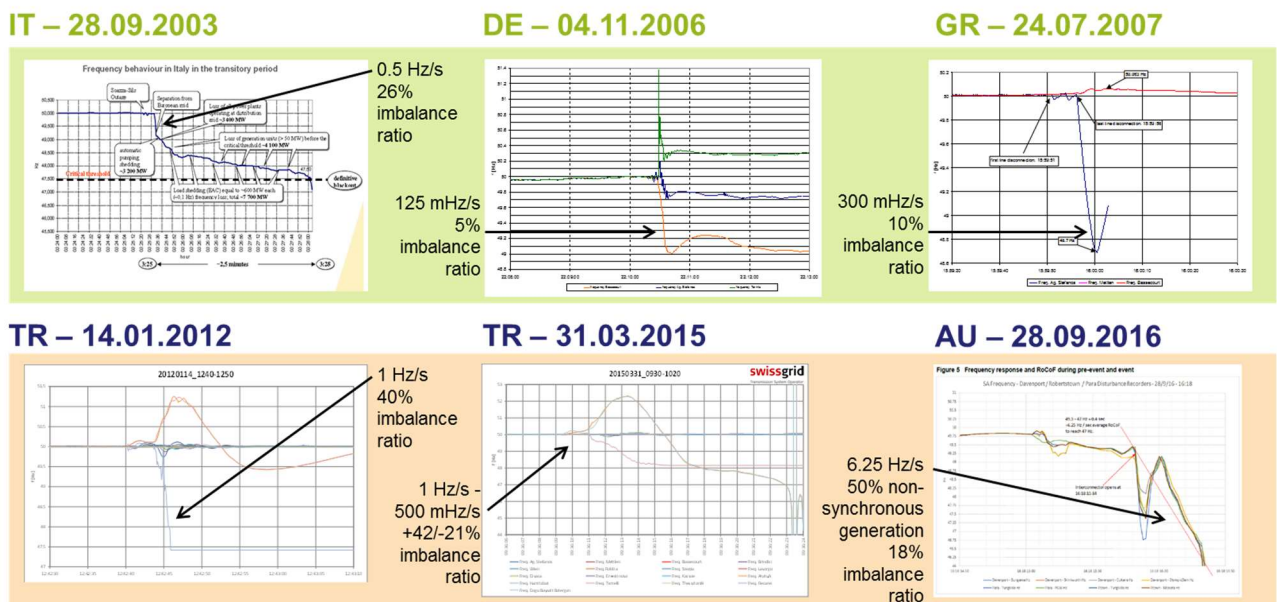


Figure 24 – Worldwide serious events

The lower graphs show transients with RoCoF higher than 1 Hz/s; all these events ended with fast grid collapse, due to the incapacity of regulations and defense systems to trigger in time and counteract the transient.

Therefore, we can deterministically conclude that transients with RoCoF higher than 1 Hz/s are not manageable by system protections; this limit is related to the minimum time to measure the phenomena in a stable and secure way and react by opening the circuit breakers of loads or generation. It seems that the current technology does not guarantee correct operation of protection equipment in the presence of this kind of transients.

10. Pragmatic Limit for Inertia and Rate of Change of Frequency

As the system inertia decreases, assuring the system security becomes a more challenging task for system operators. This issue has to be tackled in different time frames, from planning stages to real time operation.

Depending on these time frames, the set of possibilities is different:

- **At planning stages:** the devices and/or services needed to assure a certain level of minimum inertia in each system (or area of the system) have to be defined: i.e. synchronous condensers, storage with fast primary reserve, HVDC links able to provide frequency support capabilities, etc. In this stage, the evolution of new controls and devices (i.e. under frequency controls, grid forming-) must be followed, as they can allow a better approach to this challenge.
- **Closer to real time:** system operators should improve their capability to measure or estimate the system inertia and, therefore, the consequences of possible system events. This means that the dynamic stability assessment (DSA) must cover frequency stability problems stemming from decreased system inertia.

In any timeframe, a close coordination between system operators is needed in order to arrange solutions in an efficient way (technically and economically).

The current analysis over the capabilities of the existing and in usage frequency measurement principles shows that a total measurement and tripping time of about 120 ms must be considered for UFLS relays. By adding the circuit breaker time of approximately 70 ms for medium voltage circuit breakers, a total reaction time of 200 ms is to be assumed / [2]

11. Conclusions and Recommendations

The present document explains the complex intercorrelation of the Inertia issue with the hidden complex elements that characterize the worldwide grid during the so called “energy transition”. Short Circuit power, inertia, market rules, and climate changes are only some pieces of the complex puzzle that will shape the future system evolution.

Focusing on the specific inertia issue, we can note that several different off-line and on-line methods are under development and testing, with the aim to support the future system operation. On the other hand, ENTSO-E Subgroup System Protection & Dynamics (SPD SG) intends to develop and maintain a nodal (initial model) and a busbar model.

In order to define the minimum inertia limit, it is necessary to fix the maximum RoCoF value by considering:

- Stress on electrical machines of the system
- Loss of synchronism of large areas of system
- Potential split of the grid
- Sufficient time to measure the frequency and trip the protection equipment (including circuit breakers)

On the other hand, presently, some technological solutions can support provide inertia, e.g. synchronous condensers coupled with flying wheels, STATCOM, fast HVDC support to primary regulation.

One can be confident that technological innovations mainly based on inverter applications, like synthetic inertia and grid forming issues will contribute to inertia. It is, however, not yet possible to assume that this kind of technologies will be able to partially or totally counteract the gradual decrease of inertia.

A transparent and pragmatic evaluation of WAMS recordings shows that, due to the loss of grid control, RoCoF values exceeding 1 Hz/s are not sustainable with some of the present technology, mostly the synchronous machines and auxiliary loads/processes within thermal power plants.

It is important to underline that black-out events, like the Australian one, could be representative for the future configuration of the Continental European grid, with a significant prevalence of inverter-based generation and RoCoF around 6 Hz/s, which is clearly not sustainable.

It can be observed that from the events analysed RoCoF values exceeding 1 Hz/s in one of the subsystems have shown unstable behaviour that lead to blackout.

The evolution of the system towards less inertia and increasing transits will lead to higher RoCoF values in the resulting islands after a system split. Therefore, the ability of the system to be designed and operated against system split, together with a higher RoCoF withstand capability will have to be considered and further analysed. This must be then reflected in the Connection Network Codes, considering the necessary cost-benefit assessments too.

On the other hand, the current control and system protection schemes are not yet designed and capable to stabilize the islands after a system split. Further analysis will have to be performed in order to find out to which extent this situation might be improved.

12. References

- [1] ENTSO-E SPD WG, “Analysis of CE Inter-area Oscillations of 1st December 2016,” 2017. [Online]. Available: https://docstore.entsoe.eu/Documents/SOC%20documents/Regional_Groups_Continental_Europe/2017/CE_inter-area_oscillations_Dec_1st_2016_PUBLIC_V7.pdf.
- [2] “Power System Frequency Measurement,,” FNN Statement, June, 2020.
- [3] ENTSO-E, “Continental Europe significant frequency deviations - January 2019,” April 2019. [Online]. Available: https://docstore.entsoe.eu/Documents/News/2019/190522_SOC_TOP_11.6_Task%20Force%20Significant%20Frequency%20Deviations_External%20Report.pdf.
- [4] H. P. Asal, P. Barth, E. Grebe and D. Quadflieg, “Dynamic System Studies of new Requirements, Strategy for the Primary Control,” in *CIGRE Sessions*, Paris, 2019.
- [5] “European Power System 2040 Completing the Map - Technical Appendix,” [Online]. Available: https://docstore.entsoe.eu/Documents/TYNDDP_documents/TYNDDP2018/System_Need_Report.pdf.
- [6] “Final Report System Disturbance on 4 November 2006, UCTE, January 2007,” [Online]. Available: https://www.entsoe.eu/fileadmin/user_upload/_library/publications/ce/otherreports/Final-Report-20070130.pdf.
- [7] “Report on Blackout in Turkey on 31st March 2015, PG Turkey, ENTSO-E, September 2015,” [Online]. Available: https://docstore.entsoe.eu/Documents/SOC%20documents/Regional_Groups_Continental_Europe/20150921_Black_Out_Report_v10_w.pdf.
- [8] ENTSO-E SPD WG, “Frequency Stability Evaluation Criteria for the synchronous Zone of Continental Europe,” March 2016. [Online]. Available: https://docstore.entsoe.eu/Documents/SOC_documents/RGCE_SPD_frequency_stability_criteria_v10.pdf.
- [9] ENTSO-E SPD WG, “Oscillation Event 03.12.2017,” March 2018. [Online]. Available: https://docstore.entsoe.eu/Documents/SOC%20documents/Regional_Groups_Continental_Europe/OSCILLATION_REPORT_SPD.pdf.
- [10] “Final Report of the Investigation Committee on the 28 September 2003 Blackout in Italy, UCTE, April 2004,” [Online]. Available: https://www.entsoe.eu/fileadmin/user_upload/_library/publications/ce/otherreports/20040427_UCTE_IC_Final_report.pdf.
- [11] ENTSO-E, “ENTSO-E dynamic model,” 2015. [Online]. Available: <https://docstore.entsoe.eu/publications/system-operations-reports/continental-europe/Initial-Dynamic-Model/Pages/default.aspx>.
- [12] ENTSO-E SPD WG, “Frequency Measurement Requirements and Usage,” January 2018. [Online].
- [13] “Wide area monitoring systems – support for control room applications,” in *CIGRE TB 750*, Dec. 2018.
- [14] “Determining generator fault clearing time for the synchronous zone of Continental Europe,” 3 February 2017. [Online]. Available: <https://eepublicdownloads.blob.core.windows.net/public-cdn-container/clean->

documents/SOC%20documents/Regional_Groups_Continental_Europe/2017/SPD_FCT-BestPractices_website.pdf.

